To the Graduate Council:

I am submitting herewith a thesis written by Teodros Belay entitled "An Optical Real-Time, Noncontact Vibration Measurement Technique." I have examined the final copy of this thesis for form and content and recommend that it be accepted in the partial fulfillment of the requirements for the degree of Master of Science, with the major in Engineering Science.

Thomas G. Carley

Thomas G. Carley, Major Professor

We have read this thesis and recommend its acceptance :

W M Breazeale

Joseph A. M. Boulet

Accepted for the council:

C W Minkel

Vice Provost
and Dean of The Graduate School

STATEMENT OF PERMISSION TO USE

In presenting this thesis in partial fulfillment of the requirements for a Master's degree at The University of Tennessee, Knoxville, I agree that the Library shall make it available to borrowers under rules of the Library. Brief quotations from this thesis are allowable without special permission, provided that accurate acknowledgment of the source is made.

Permission for extensive quotation from or reproduction of this thesis may be granted by my major professor, or in his absence, by the Head of Interlibrary Services when, in the opinion of either, the purpose of the material is of scholarly purpose. Any copying or use of the material in this thesis for financial gain shall not be allowed without my written permission.

Signature Teodros Belay

Date July 31st 1987

AN OPTICAL REAL-TIME, NONCONTACT VIBRATION MEASUREMENT TECHNIQUE

A Thesis
Presented for the
Master of Science
Degree
The University of Tennessee, Knoxville

Teodros Belay

August 1987

To my parents

ACKNOWLEDGMENTS

I am indebted to Professor T. G. Carley for his invaluable guidance and Professor H. Pih for letting me use his laboratory and equipment. I am also indebted to Professor M. A. Breazeale for his stimulating discussions throughout my undergraduate and graduate curriculum, and to Dr. J.A.M. Boulet who served on my thesis committee.

I am grateful to my parents Belay Redda and Hiwot Nėmariam for their relentless support. Without the moral support of Alem Belay, Algetta Belay, and Solomon Belay the completion of this thesis would have not been possible. Last but not least thanks are due to Misrak Million for her support and partially typing the manuscript, and to James R. Cain for his help with the computer in the preparation of this thesis.

ABSTRACT

Presented in this work is an optical real-time, noncontact vibration measurement technique that measures vibration amplitudes above the shadow moire range (greater than 0.1 mm).

An experimental technique was devised whereby vibration amplitude measurement can be made using the modulation of reflected light from a vibrating object. A direct calibration was made for exact object displacement to detector voltage reading. By using this method the first three mode shapes of a cantilever beam were traced.

The primary conclusion of this study is that the technique is a practical vibration measurement tool with a measurement range extending from 0.1 mm to at least 10 mm.

TABLE OF CONTENTS

LIST OF TABLES

LIST OF FIGURES

FIGURE PAGE

FIGURE PAGE

I. INTRODUCTION

The use of optical techniques as practical vibration measurement tools was greatly facilitated by the invention of the laser. The coherent and monochromatic properties of laser light opened a new avenue in the investigation of many phenomena including vibration. Optical techniques such as moire, holography, and speckle interferometry all been used to measure phase and amplitude of a vibrating object. Optical techniques such as those mentioned above are of great use because they do not require mechanical contact with the object while investigating its vibrational properties. Although the production of superimposed dark and bright fringes make the determination of vibration amplitude possible for the three techniques, none of them can be used to study the actual movement of an object as a function of time. To this end, Kafri et al. [1] and Dirckx et al. [2] have addressed the problem and demonstrated time history measurement using the projection moire technique and the shadow-moire technique respectively.

Kafri makes use of a Ronchi ruling and casts a shadow of the ruling onto an object. A photograph, taken at some angle to the ruling, is processed to obtain a positive transparency of the projected grating. When this transparency is placed at the back of the camera, the image which is transmitted through the transparency to the camera's focal plane is a superposition of the object (with the grating projection on its surface) and the transparency [1]. Any displacement of the vibrating object results in a fringe pattern at the focal plane which is produced by the difference in position between the object at rest and the distorted object [1]. By making use of a photodetector to view the above, Kafri et al. demonstrated that the out of plane motion of a vibrating object can be measured in real time. Dirckx et al., on the other hand, casts a shadow of a square wave grating onto an object. This produces shadow-moire fringes which can be viewed when observing the projection of the grating through the grating itself [2]. The space behind the grating is thought of as an arrangement of dark and bright fringe planes. If a point on an object is moving back and forth between these planes a photodetector tracing this movement indicates a varying intensity pattern with a corresponding voltage reading. This voltage is directly calibrated to a known object movement. Calibration is achieved by mounting the object on a translational stage and recording the output voltage versus displacement when the object is translated. This is done within the approximately linear range of the sinusoidal intensity pattern between the dark and bright fringe planes. If a vibrating point moves across one of these planes there will be a dip in the detector signal and thus an accurate calibration is not available for this case. The linear profile may be extended by reducing the angle of illumination and observation or by using a coarser grating to study larger movements. With such adjustment the upper displacement range of this technique is 0.1 mm. The lower displacement range can be extended to 100 nm by using a lock-in amplifier in the detection process. To make vibration amplitude measurement of a point, Dirckx used a small piece of grating with an area of about 4 sq mm. The work of Dirckx differs from Kafri's in that Dirckx's technique has no time delay caused by film development and no photomultiplier is needed.

The work discussed herein involves the development of a technique that is used to study movement of an object as a function of time. The measurement of vibration amplitude of a point on an object is made. The basis of this technique stems from Dirckx's work, but is quite different from it. The similarity of the technique discussed herein to Dirckx's is found in the calibration of voltage to displacement. Both techniques make use of the object mounted on a translational stage. The object is translated a known distance between dark and bright planes within the approximately linear range. For a given translation there will be a corresponding voltage change and, by recording these data, voltage change is directly calibrated with respect to a known object movement. The difference is that this method does not require the generation of moire fringes, thus eliminating the need for a grating, a lens, and an op-amp. This fact introduces some limitations and opens up possibilities which will be discussed subsequently in this text. The technique developed herein was used to trace the first three mode shapes of a vibrating beam.

II. BASIC CONCEPT

In studying the movement of an object as a function of time, Dirckx's method requires the generation of shadow-moire fringes. The space between the object and the square wave grating placed in front of it is thought of as being filled with parallel bright and dark fringe planes. The intensity between these planes varies sinusoidally with a portion of the range being approximately linear. When an oscillating point on an object is placed within this linear range, it is possible (using a photodetector) to get a trace of the object's motion. By calibrating voltage change to a known object movement within the linear intensity range, one can obtain amplitude measurement of a vibrating point. The dynamic range of Dirckx's method is thus determined by the spacing of bright and dark fringe planes and the sensitivity of the linear range of the intensity profile. Dirckx points out that the maximum amplitude that can be measured using the shadow-moire technique is 0.1 mm. This fact introduces a limitation to the application of this technique for objects vibrating with an amplitude of greater than 0.1 mm. If one wishes to have a noncontact method such as Dirckx's that deals with vibration amplitudes greater than 0.1 mm, the next logical step is then to try to extend the amplitude range. As was mentioned earlier, it is the spacing between the dark and bright fringe planes, or more specifically, the distance from a maximum to minimum point of the linear range within the sinusoidal intensity profile, that restricts the amplitude range. This implies that if one could extend the width of the linear range, one would be able to measure amplitudes greater than 0.1 mm.

This problem can be addressed in the following manner. Consider a finite width laser beam illuminating a reflective surface at an angle. The reflected light is contained in an envelope that would ideally extend to infinity as shown in figure 1. The laser beam has a Gaussian intensity distribution [3]. Hence, if a cross section parallel to the reflective surface is taken at any distance relative to the reflective surface it would have a near Gaussian intensity distribution. The scattering that occurs at the reflecting surface expands the distribution depending on where the cross section is from the reflective surface. Consider that this reflected light is viewed in a dark room. In this case, one may effectively think of the bright spot from the reflected light and the dark room as one bright plane and two dark planes. If a cross section of these planes is taken parallel to the reflective surface, a bright spot and two dark spots on either side of the bright spot are formed along the cutting plane as shown in figure 2. The space between the bright and dark points varies continuously in intensity and it is of Gaussian distribution. When the illuminated point P, shown in figure 2, moves back and forth normal to the surface, the bright and dark spots move back and forth along the cutting plane. In a restricted range between the maximum and minimum intensity the variation of intensity is approximately linear. This intensity pattern is investigated in chapter 4 in detail. The linear range is located midway between the dark and bright spots. In this range, the intensity

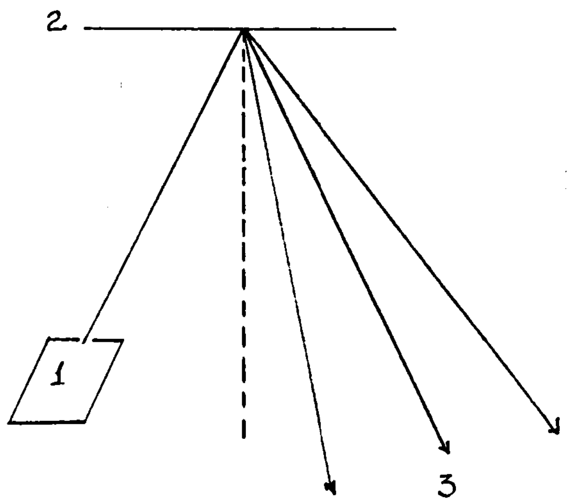

Fig. 1. Reflection from illuminated surface.

1. Light source
2. Object surface
3. Reflected light envelope

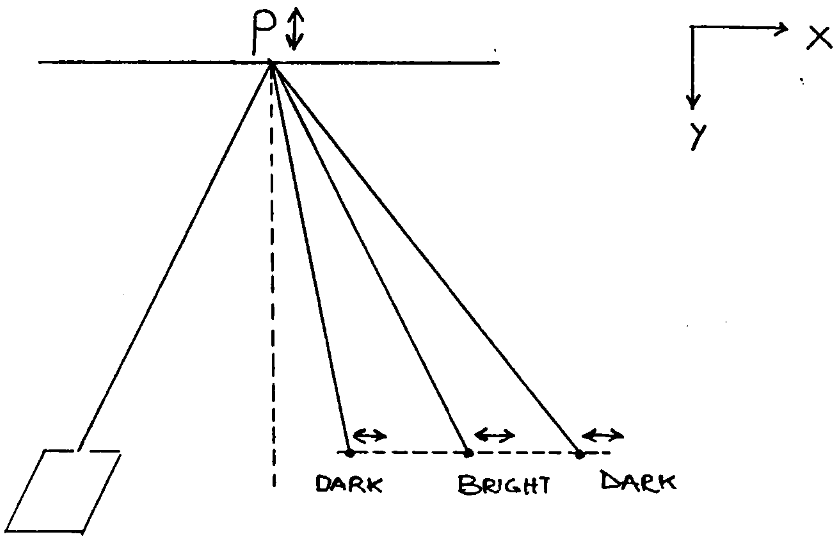

Fig. 2. Motion of point P and the bright and dark spots on the cutting plane.

changes at a maximum rate from point to point. If a small aperture detector is placed midway between the dark and bright spots (in the linear range) when point P is moving back and forth, the detector signal will show a sinusoidal pattern as in figure 3. When the amplitude of the vibrating point is large enough to cause the bright and dark spots to cross the detector, the detected signal will show a dip as in figure 4a. If the detector is placed anywhere near the dark spot the detected signal will show a pattern as in figure 4b. Since the intensity variation between the dark spots is of Gaussian distribution, one can not use the appearance of a dip (figure 4a) to calibrate the system. This is because such calibration assumes a linear intensity profile. Therefore, a different approach must be taken to get a direct calibration between a known object movement to detector voltage output. The calibration procedure is discussed in chapter 4.

Figure 3 shows a detected signal with a sinusoidal pattern. A shaker was used to induce vibration of a cantilever beam. The applied driving current was sinusoidal, thus the detected vibration pattern was also sinusoidal. If a point (such as P in figure 2) is driven by a signal other than sinusoidal (asymmetric, random, ...) the object movement may still be detected. To demonstrate this, a thin rectangular membrane (aluminum foil) taped on a screen (with a rectangular hole cut out at the center) was excited by music (a nonperiodic driving source) as shown in figure 5. When the center of the membrane is illuminated by a point source, the point's motion is observed by the detector whose output voltage is shown in figure 6. This trace shows varying peaks

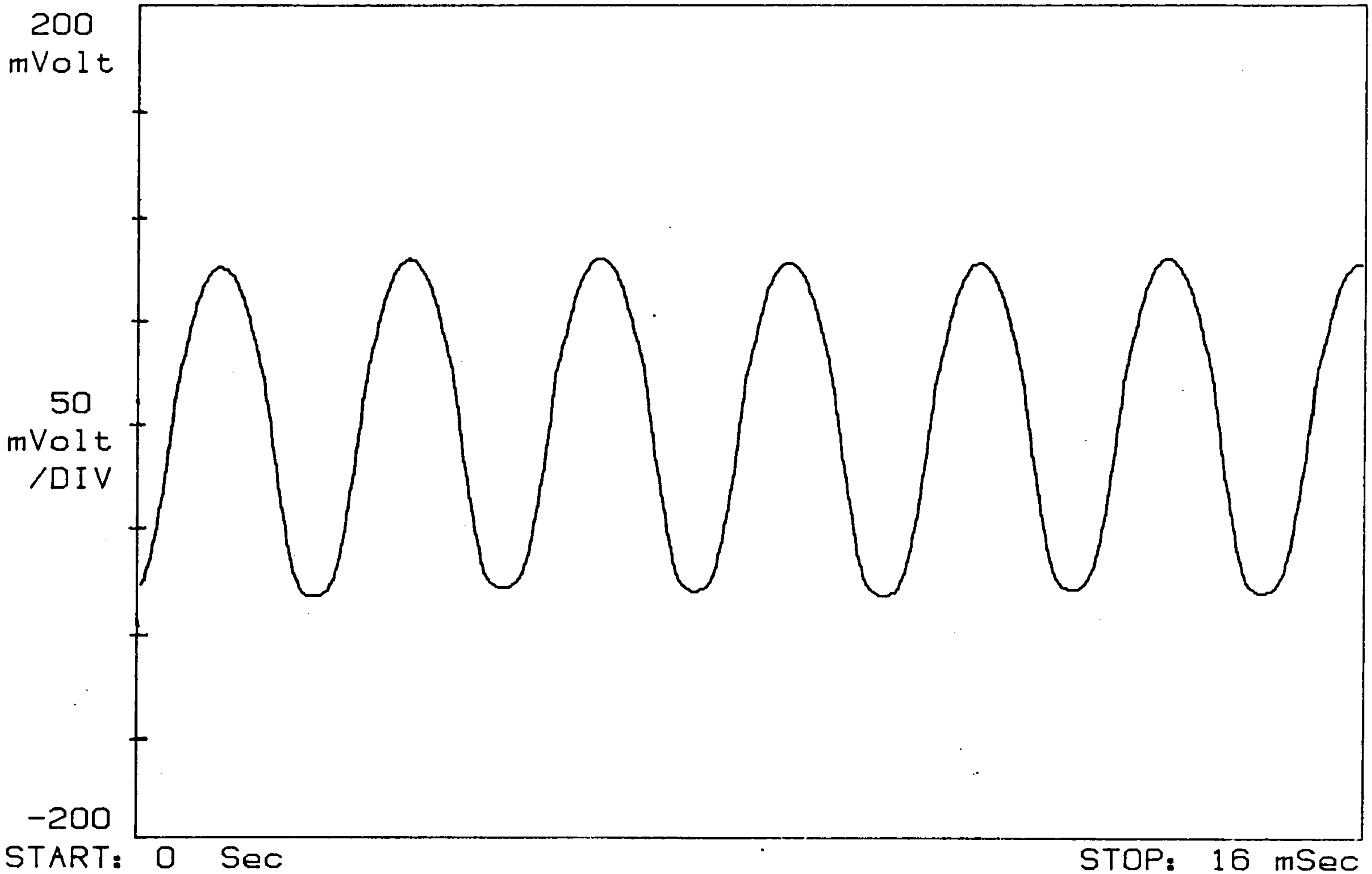

Fig. 3. Detector signal for the motion of point P.

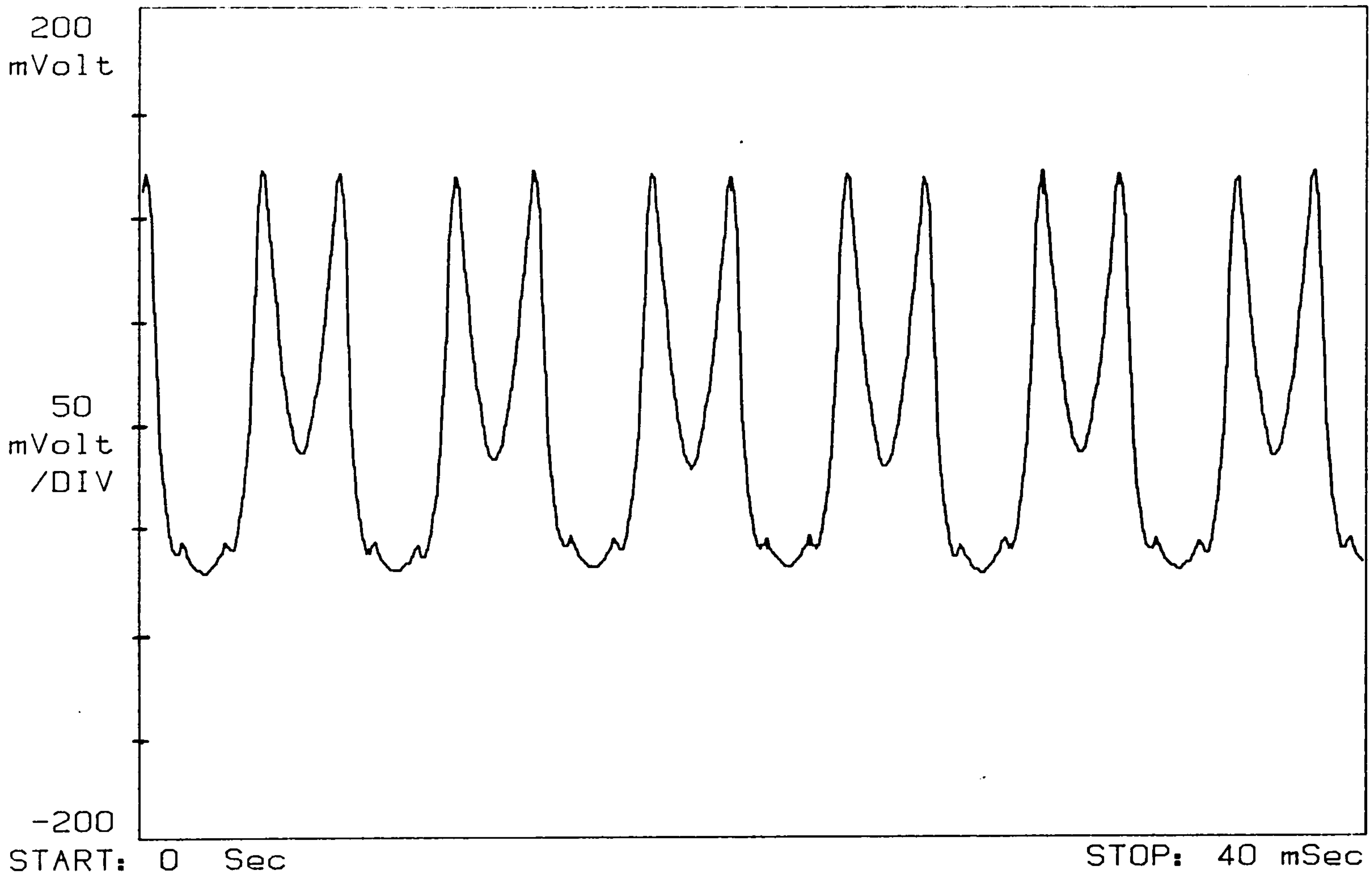

(a) detector signal when amplitude of point P is large

Fig. 4. Effects of detector position on signal traced.

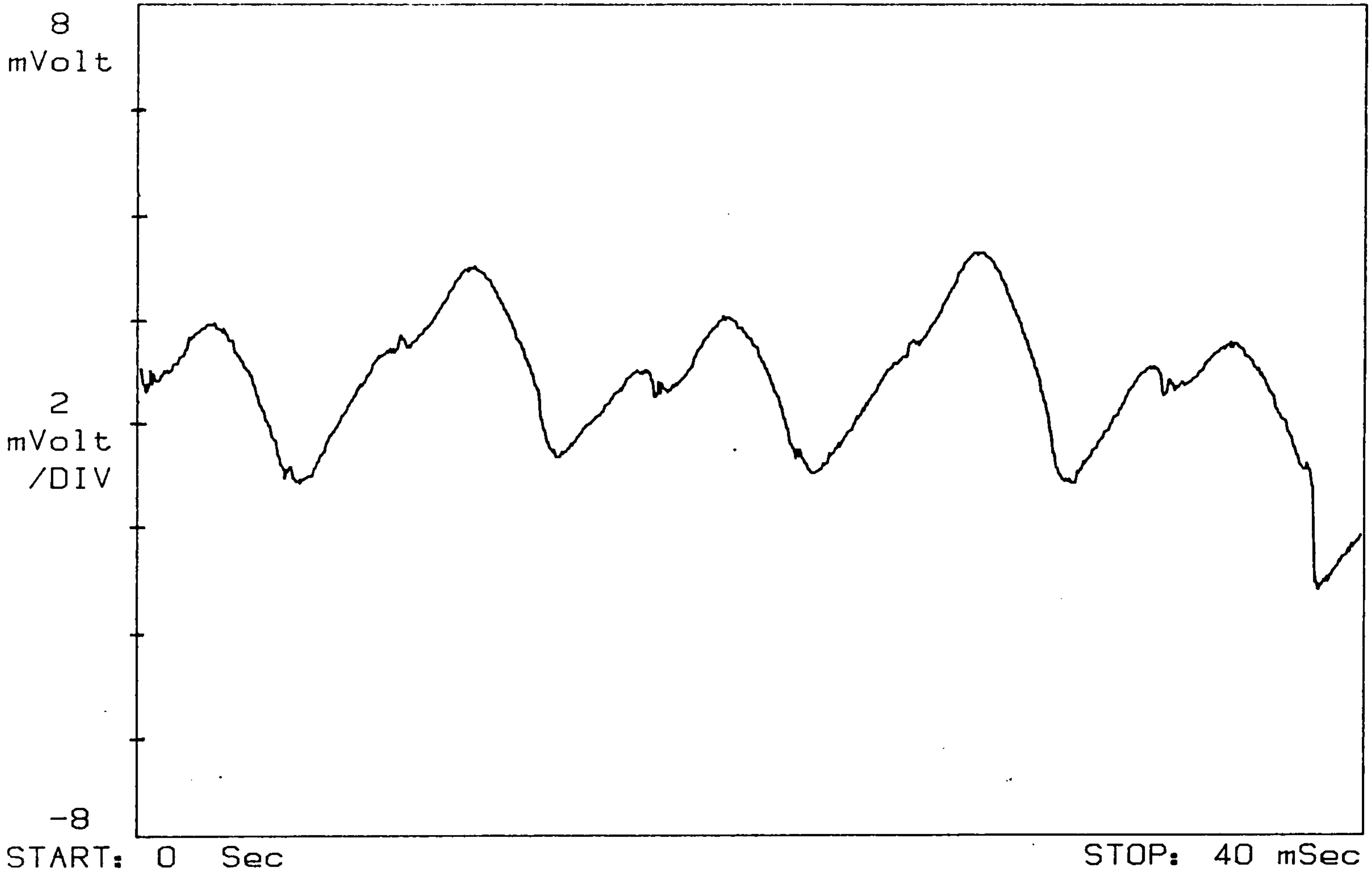

(b) detector signal when detector is placed near the dark spot

Fig. 4 (continued)

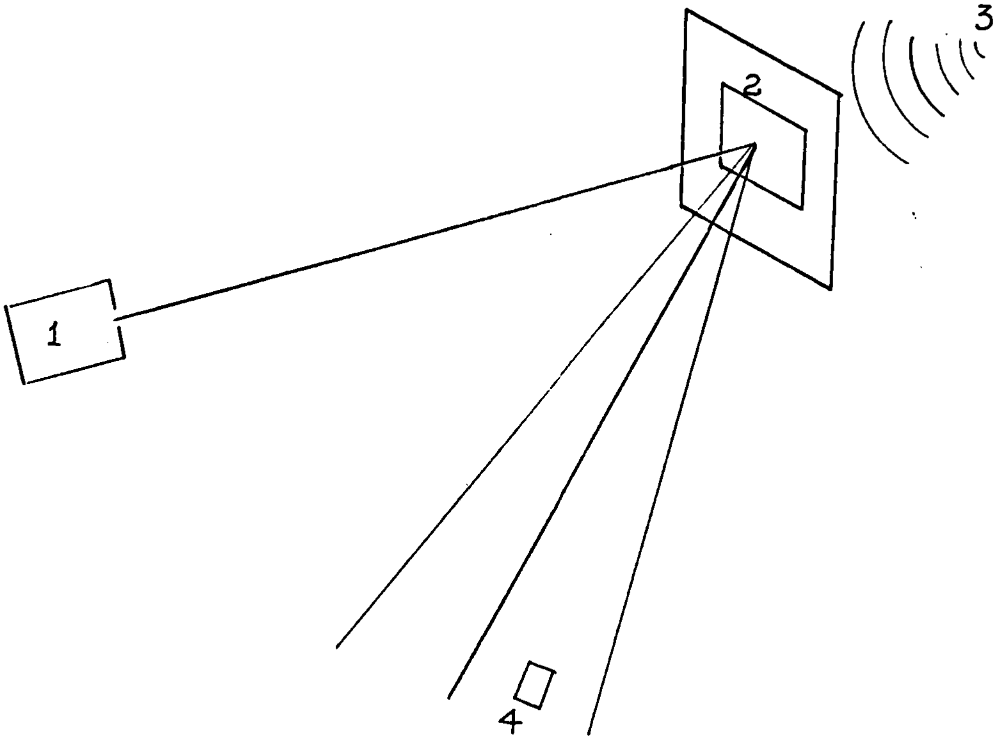

Fig. 5. Experimental setup to observe membranes motion at a point.

1. Light source
2. Membrane
3. Acoustic wave
4. Photodetector

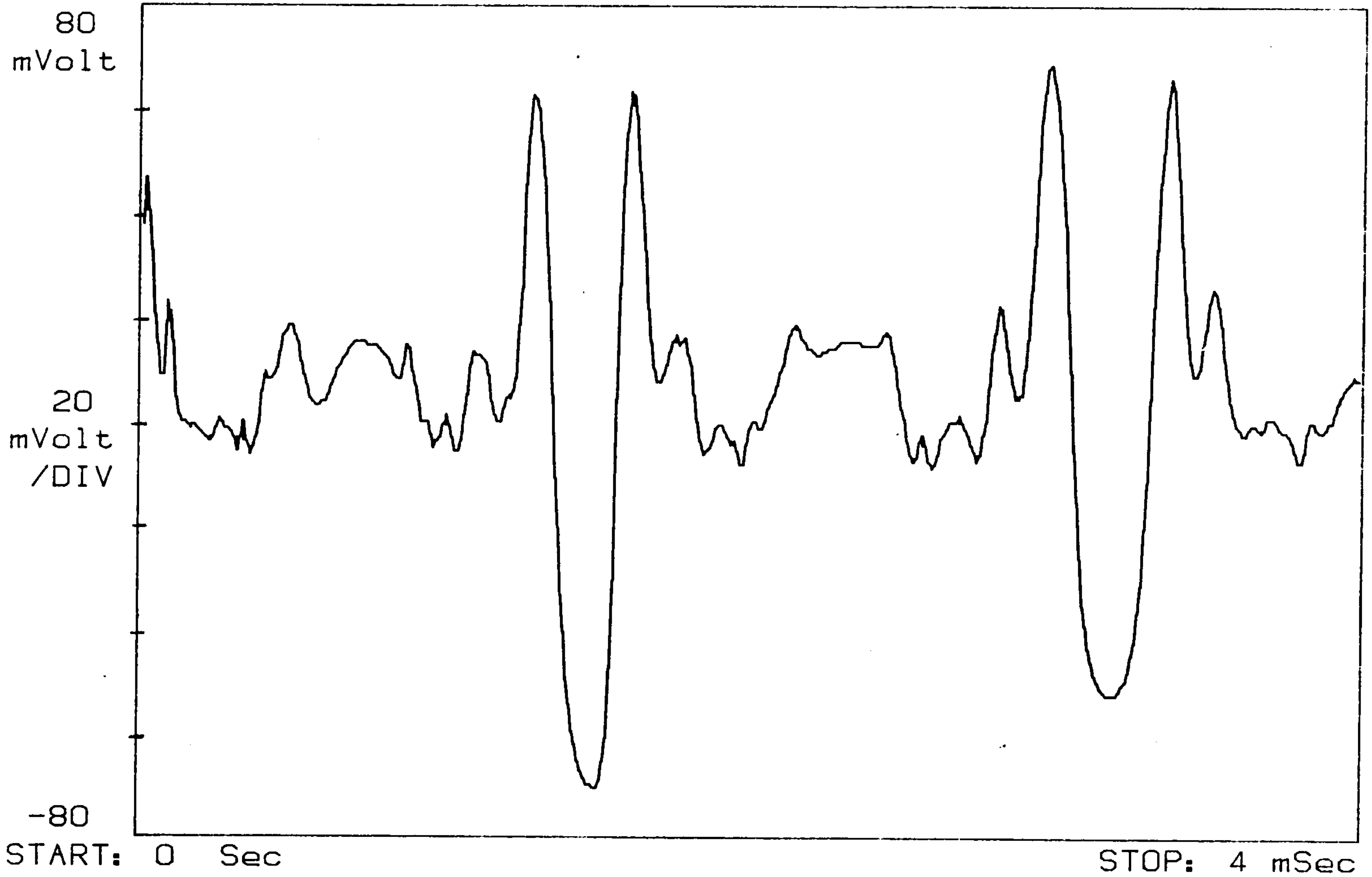

Fig. 6. Detector signal for the motion of a point when the membrane is excited by a nonperiodic signal.

which correspond to certain sound intensity levels, that is the larger peaks correspond to higher intensities observed by the motion of the illuminated point.

To show the feasibility of the above concept as a practical vibration measurement tool, a cantilever beam was used and its first three mode shapes were traced using this technique. In the following chapters the experimental setup, calibration technique, and the results of implementing this technique will be discussed.

III. CONCEPT APPLICATION

Experimental Setup

A single experimental setup is used to calibrate the system and to trace the mode shapes of a cantilever beam. Figure 7 shows a top view of the experimental setup. This setup is situated in a sufficiently dark room to facilitate the dark to bright contrast needed between the reflected light and the surroundings. The chopper (12) in front of the illuminating beam is used for calibration purposes, which will be discussed in the following chapter. A Spectra-Physics Stabilite 0.5 mW He/Ne laser source (2) is used to illuminate a point on the vibrating beam (11). The laser beam cross section diameter is 3 mm. Thus, when a point is referred to in this text, it has a diameter of 3 mm. The laser may illuminate a point at an arbitrary angle between 0 to 90 degrees measured from the y-axis (see figure 7). In this experiment a 14 degree angle was chosen. A more detailed explanation as to why this is done is given on page 28. The illuminated vibrating beam, with a strip of reflective tape attached to enhance reflectivity, is made of aluminum 6061-T6. Its dimensions are shown in figure 8. The beam is excited by a Delta Dynamics 501-10 shaker (8) which is driven by a Systron Donner 415 function generator (9). Vibration amplitudes near the clamped edge of a cantilever beam are small. Hence, the shaker is placed near the clamped edge so that the shaker's input amplitude does not limit the response of the beam at the shaker input point. The shaker is attached 15 cm from the clamped end. The reflected laser beam is detected by an EG&G Light Mike (5) with a sensitive detector area of 1.28 sq mm. The

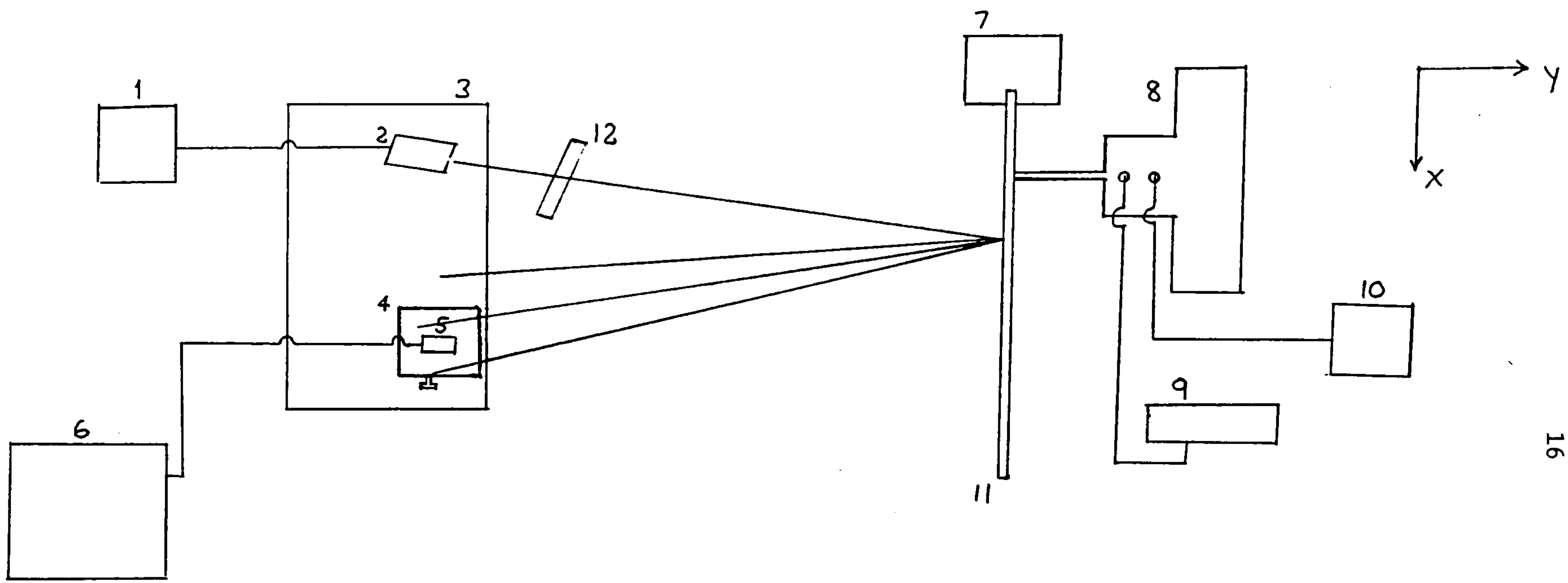

Fig. 7. Experimental setup.

1. Laser power source
2. 0.5 mW He/Ne laser
3. Translational stage
4. Precision translator
5. EG&G lite mike
6. HP 3561A signal analyzer
7. Clamp
8. Shaker (Delta Dynamics 501-10)
9. Systron Donner 415 Function Generator
10. 6 volts power supply
11. Vibrating beam with a reflecting tape
12. Chopper

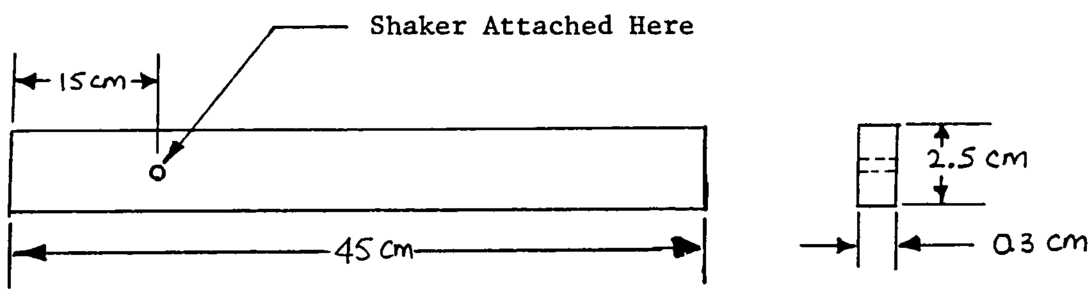

Fig. 8. Test specimen, AL 6061-T6.

detector is placed on a precision translator (4). This is done to avoid displacing the object and thus disturbing the clamped edge in an attempt to calibrate the system. Instead, from the relationship that exists between beam displacement and detector displacement (discussed in chapter 4), it is only necessary to displace the detector to calibrate the system. The signal from the detector is sent to an HP 3561A signal analyzer (6). The analyzer shows a trace of the object's motion and provides a proportional voltage reading. The laser and the detector are both placed on a translational stage (3). The orientation of this stage is parallel to the vibrating beam and free to move parallel to the beam. This stage is used to move the laser and the detector, at the same time, leaving their orientations with respect to the vibrating beam undisturbed in the course of tracing the mode shapes.

Procedure

The purpose of the experimental setup is to measure vibration amplitudes of different points on a vibrating beam thereby tracing a particular mode shape. Arbitrary points on the vibrating beam are marked as shown in figure 9. The laser and detector are positioned on the translational stage (see figure 7) as determined from the calibration procedure discussed in the next chapter. Point 0 shown in figure 9 is illuminated by the laser beam while it is vibrating. The detector monitors the vibration and produces a signal. This signal is sent to the HP analyzer where a trace of the object's motion with a corresponding voltage is displayed. The voltage reading is stored. At the proper time, the voltage is converted to vibration amplitude from the

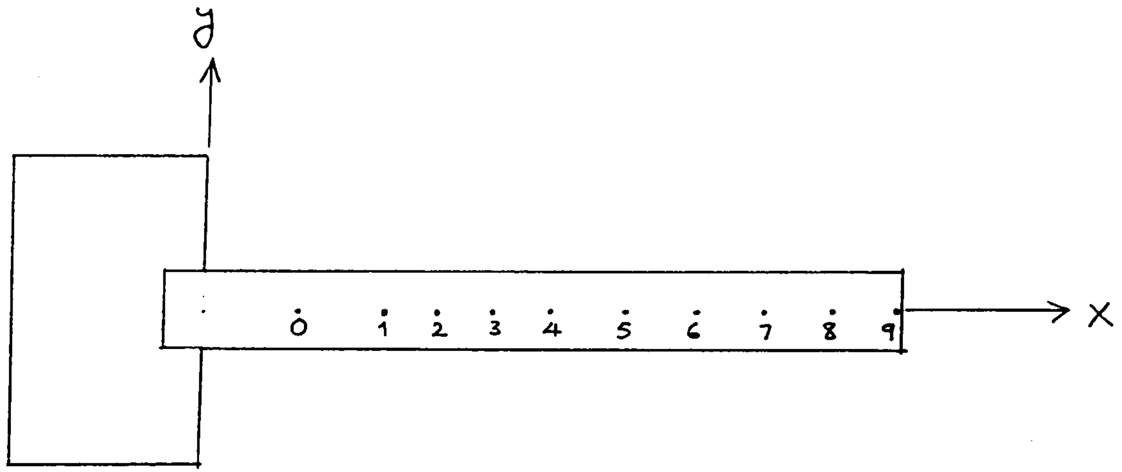

Fig. 9. Measured points on cantilever beam: distances from x-axis.

0 = 13.5 cm
1 = 16.5 cm
2 = 19.9 cm
3 = 24.6 cm
4 = 28.0 cm
5 = 31.2 cm
6 = 34.7 cm
7 = 38.3 cm
8 = 41.8 cm
9 = 44.9 cm

relation obtained by the calibration procedure. The stage (see (3) figure 7) is now translated in the positive x-direction until the laser beam illuminates point 1 in figure 9. The subsequent voltage measurement is made and the voltage reading is stored. By following this procedure the voltage measurements of all ten points in figure 9 are made. To get traces of the first three mode shapes, the beam was vibrated at the first, second, and third mode frequencies found by sweeping the function generator from zero Hz until the beam resonates at each resonant frequency.

IV. CALIBRATION

An important feature of an experimental method lies in the simplicity interpreting its data to get the desired information. Consequently, a simple calibration technique is sought for the method discussed. A procedure that relates voltage change to a known object movement has been devised.

It was mentioned in chapter two that the reflected light (see figure 1, p. 6) is spread into an envelope of varying intensity. It was claimed that the reflected light had a Gaussian intensity distribution. This can be verified by placing a photodetector in front of the reflected light. By translating the detector the intensity pattern is recorded.

Consider a laser beam incident on a point P at an angle q as shown in figure 10. The angle of reflection is equal to the angle of incidence. If the point P is moved a distance A in the x-direction, then the point of maximum intensity of the reflected light will move a distance R,

$$R = 2\ A\ \tan(q) \tag{1}$$

in the y-direction, as shown in figure 11. This indicates that when a detector is placed in front of the reflected light and translated a small distance R (to trace the intensity pattern), this movement is equivalent to a proportional object displacement A,

$$A = R\ /\ [2\ \tan(q)], \tag{2}$$

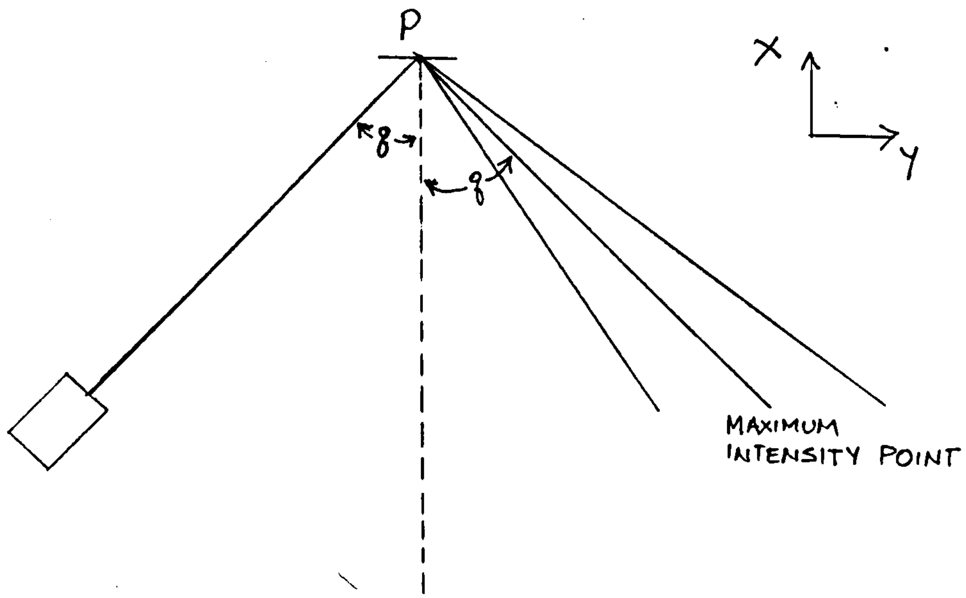

Fig. 10. Illumination and reflection angles.

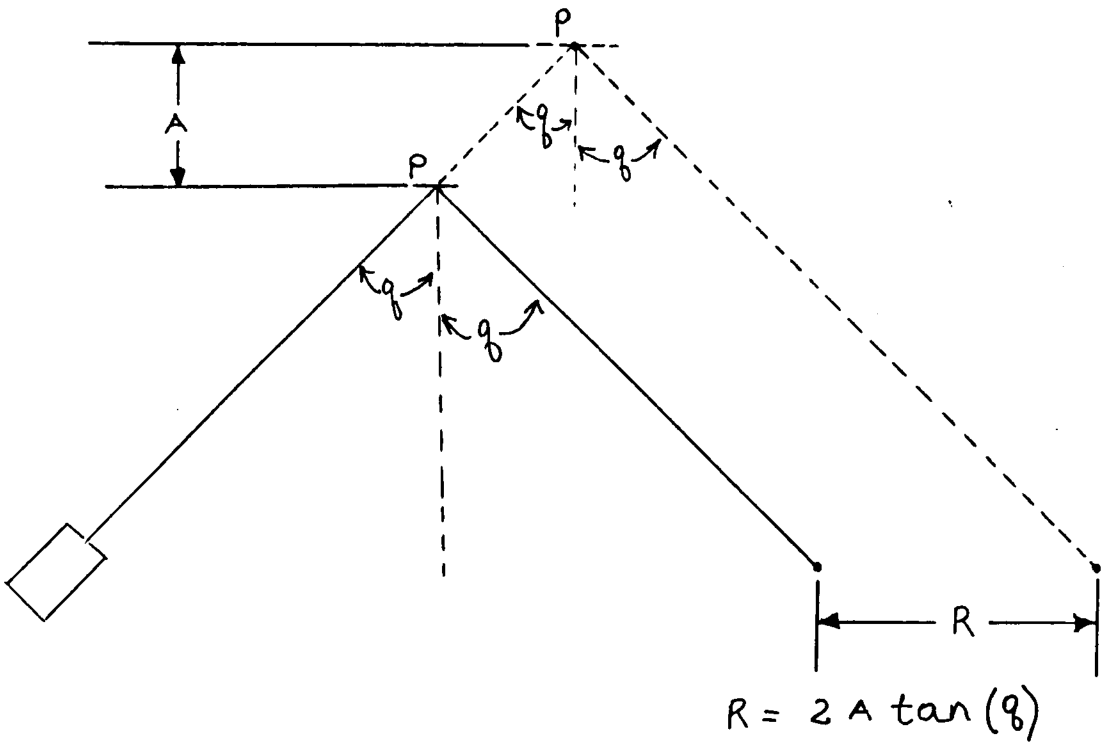

Fig. 11. Relationship between illuminated and maximum intensity point movement.

obtained from equation (1). With this in mind, the detector is placed at the point of maximum intensity of the reflected light as shown in figure 7, p. 16. A chopper is introduced in front of the illuminating laser beam. The chopper is used because the signal analyzer has an ac coupling capacitor. When the light is chopped at a frequency higher than the circuit frequency of the ac coupling capacitor, then it is possible to detect a voltage change (in the detected signal) when the detector is translated a small increment. Without the chopper, when the detector is displaced a certain increment, the circuit will detect a step change in the input signal. Thus, the circuit's response is a step change of voltage which drifts back to zero at a rate defined by the circuit's time constant. With the aid of the chopper, the detector's signal is displayed on the analyzer along with a voltage reading for the intensity of the reflected light at the maximum intensity point. Figure 12 shows the maximum intensity signal obtained from the detector. The detector is translated at small increments and the corresponding voltage readings are recorded up to the minimum intensity point. Figure 13 shows the minimum intensity signal obtained from the detector. In this manner, the intensity pattern of one side of the reflected light lobe is traced. The intensity pattern recorded for the left side of the maximum intensity point is shown in figure 14. Figure 14 is one-half of a Gaussian shaped curve with an almost linear range near the center. In tracing the intensity pattern, for each detector increment R there is a proportional object displacement A given by equation (2). This implies that, the abscissa of figure 14 can be converted into effective object

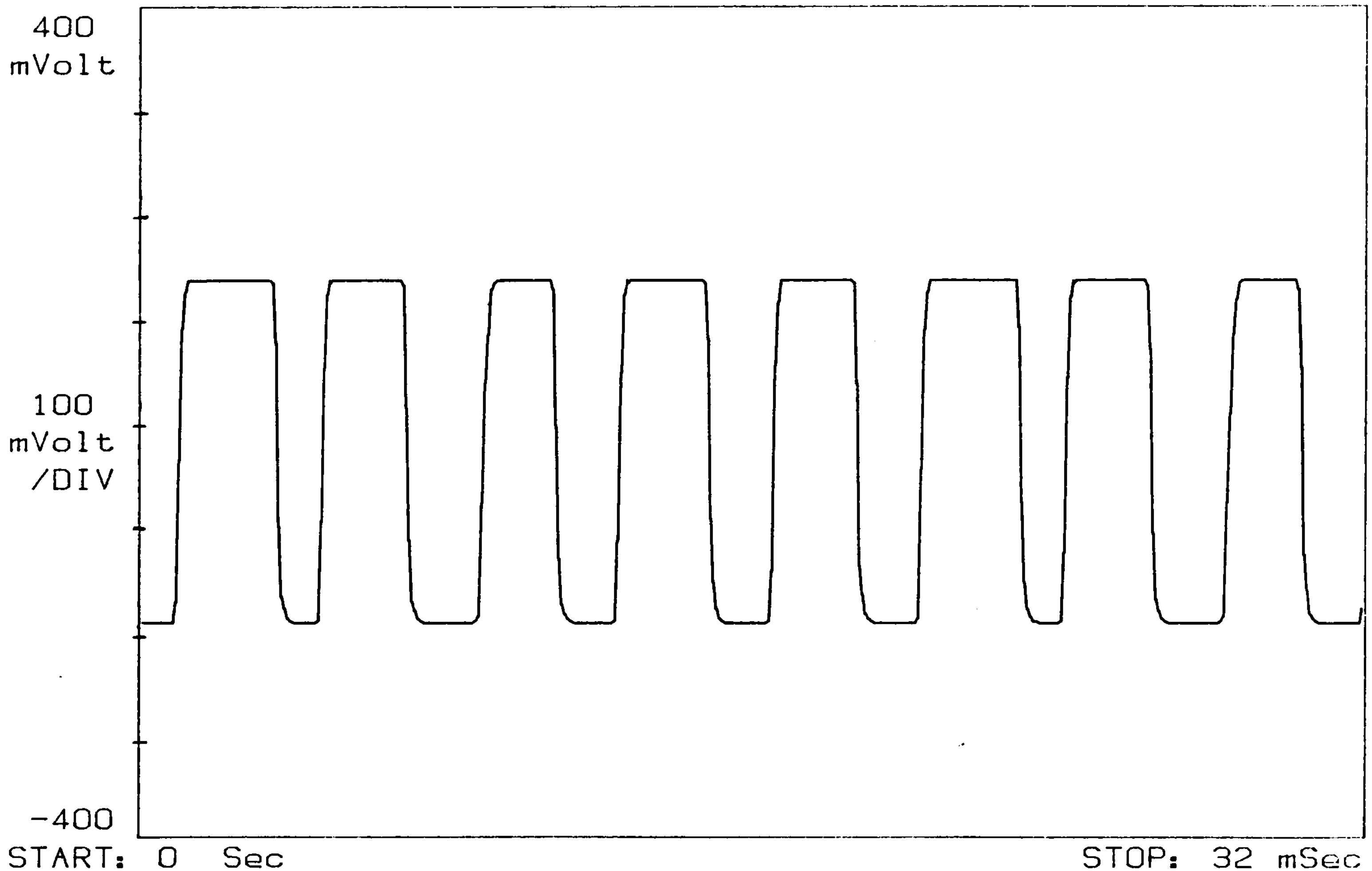

Fig. 12. Maximum intensity signal.

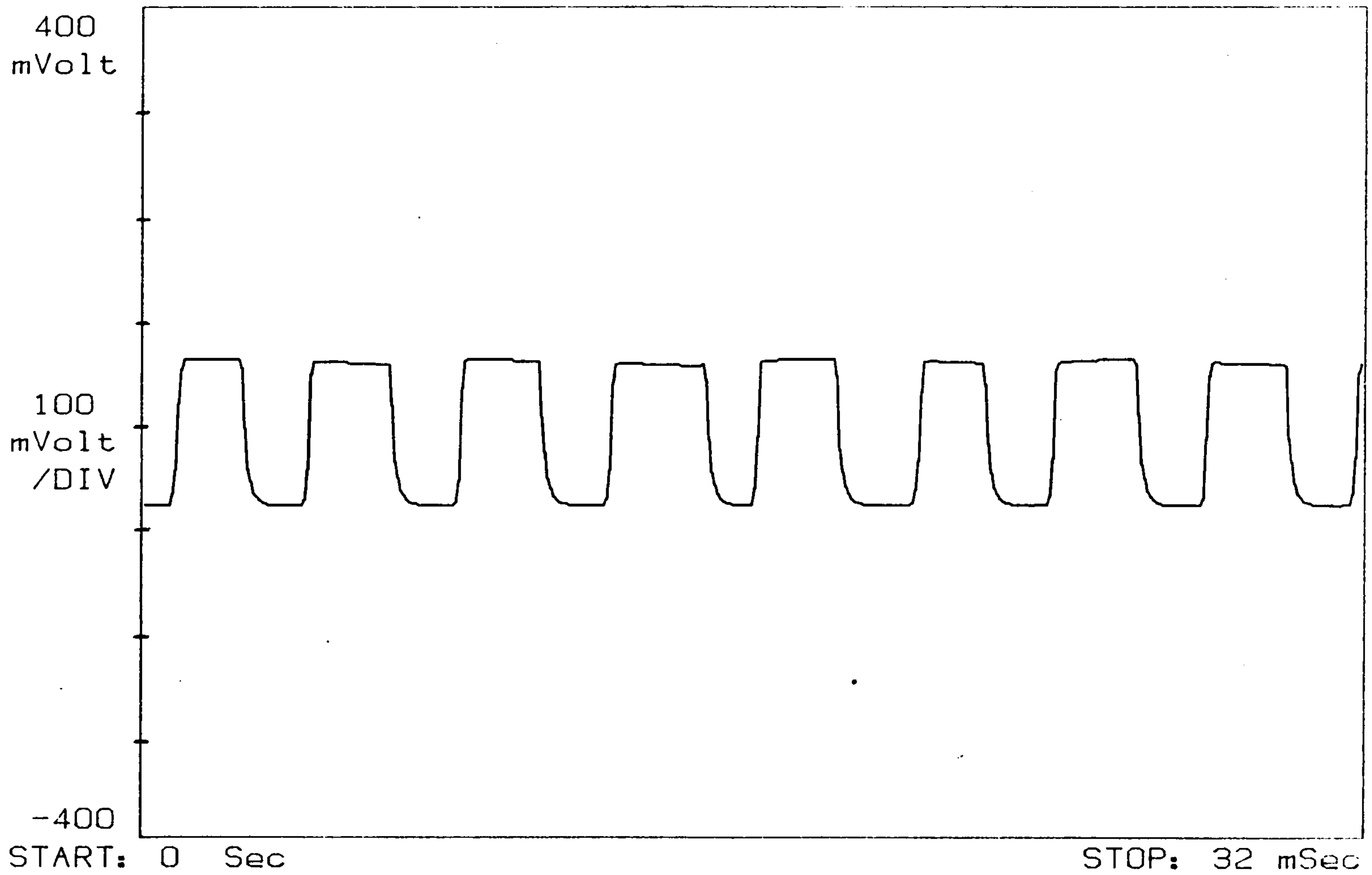

Fig. 13. Minimum intensity signal.

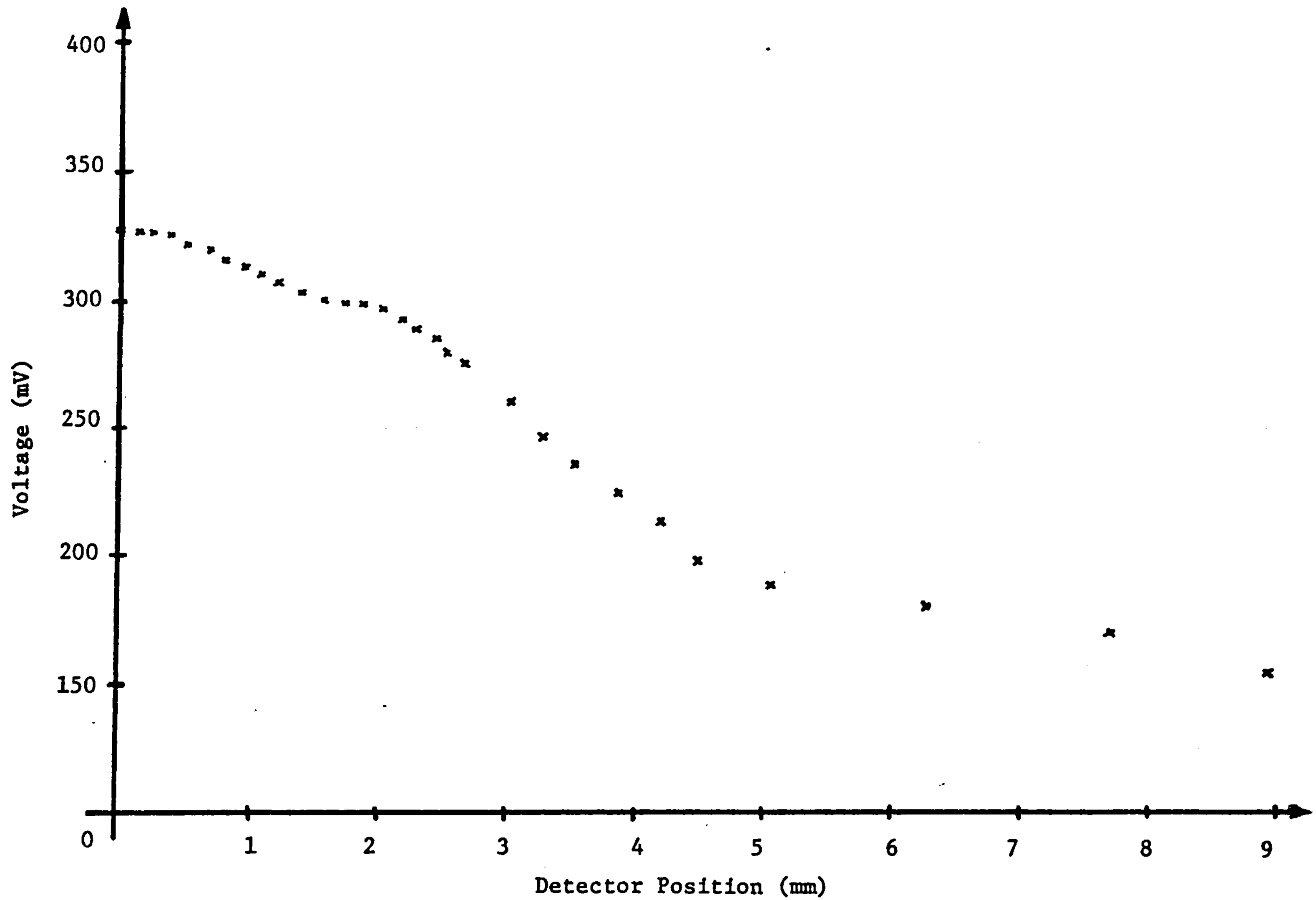

Fig. 14. Intensity pattern of the left-side of the reflected light.

displacement. Since the angle of illumination was chosen to be 14 degrees (discussed in chapter 3), the detector displacement is half the object displacement given by equation (2). Figure 15 shows a plot of intensity vs object displacement. This provides a calibration of detector voltage with respect to a known object movement. To establish a linear relationship between voltage change and displacement, only the linear part of figure 15 is used for calibration. Since the reflected light has this linear range, it is not necessary to plot the intensity pattern whenever calibration is needed. Rather, the following procedure can be used for a quick calibration.

The detector (see figure 7, p. 16) is translated until maximum intensity of the reflected light is obtained. The intensity and the detector position are recorded. The detector is displaced towards the minimum intensity, the intensity and detector position are recorded. The midposition between these maximum and minimum intensity positions is the center of an almost linear part of the intensity pattern. To calibrate the system, the detector is placed in the midposition and it is moved a small distance on either side of the central position. Both positions and the detector voltage readings are recorded. In this way, the detector voltage is directly calibrated to a known object movement. It is important to note that the application of this method is simplified because none of the instrument constants such as: laser beam to object distance, object to detector distance, and angle of illumination have been used in the calibration process. However, the angle of illumination plays an important role in the application of this method.

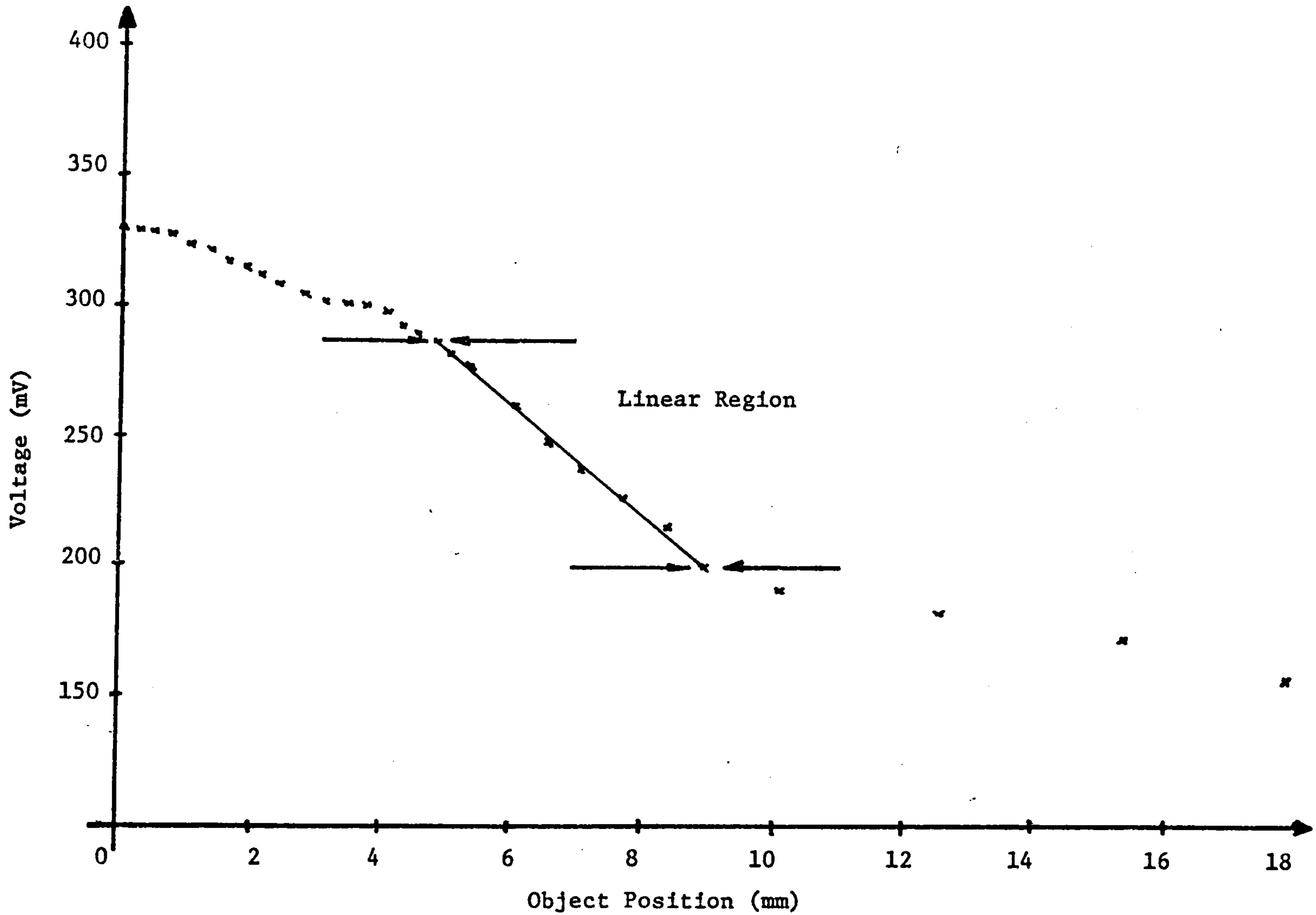

Fig. 15. Calibration curve.

When the angle of illumination q is 26.5 degrees, the distance R is equal to distance A as given by equation (1). When q is less than or greater than 26.5 degrees, the value of R is less than or greater than A respectively. The significance of q is in its effect on R which limits the amplitude range to be measured. To clarify this point, consider the setup of figure 7, p. 16, for the measurement of vibration amplitude of an object. The proposed calibration is done (for a certain angle of illumination q) and the detector is placed in the midposition of the linear range. Let the linear range have a span of X mm, and let an illuminated point on the object vibrate at an amplitude of A mm. For this case, the reflected light will be oscillating within a range of R mm given by equation (1). If R is less than X, the vibration amplitude can be measured because it would fall within the linear range of the calibration curve. If R is greater than X then the characteristic dip described in chapter 2 will appear. A calibration for this case is not available. However, the relationship that exists between q and R can be used to avoid the occurrence of the dip. If the angle of illumination is increased or decreased, R would increase or decrease respectively. The dip may then be avoided by decreasing the angle of illumination. Whenever the angle of illumination is changed, the system must be recalibrated because properties of the reflected light will also change. Specifically, the slope of the almost Gaussian curve will change, thus changing the sensitivity of the linear range.

The calibration curve can also be altered by changing object to detector distance. Referring to figure 2, p. 7, it is evident that the span of the almost Gaussian intensity pattern, and thus the slope of the linear range, increases as the cutting plane is placed further away from the point P. This implies that the amplitude measurement range can be improved by placing the detector at a suitable distance from the vibrating object. For a fixed detector to object distance the following is what limits the maximum amplitude that can be measured. The maximum value of R for a fixed value of q is determined by the properties of the light beam and the reflectivity of the object. As q is increased the maximum value of R increases. There will be a critical value of q in which the quotient (maximum R)/2tan(q) is maximized. The maximum value of this quotient is the maximum amplitude that can be measured.

V. RESULTS AND CONCLUSIONS

Calibration

The data for detector position along with the corresponding voltage reading are presented in Table 1. The detector position is converted to proportional object movement using equation (2) given on page 24. These data are plotted in figures 14, page 27, and 15, page 29, for the intensity pattern and calibration curve, respectively. The linear range of the calibration curve has a slope of 21.66 mV/mm. By using this calibration, the vibration amplitude range is 0.379 mm to 8.0 mm for this particular setup. The traces for the upper and lower ranges are shown in figures 16 and 17 respectively. These ranges are valid only for this particular experiment. As discussed in chapter 4, changing the angle of illumination or changing the detector distance from the vibrating beam changes the slope of the calibration curve and thus changes the amplitude range.

Mode Shapes

The 12 Hz input signal used to excite the first mode shape is shown in figure 18. Traces from the detector signal for each point in figure 9, p. 20, are shown in figures 19 through 23. Using the calibration (21.66 mv/mm), the voltage reading for each point is converted to vibration amplitude. The data for this mode shape are presented in Table 2. From the data of table 2 the first mode shape is drawn in figure 24. This mode shape correlates well with the theoretical first mode shape of a cantilever beam as shown in figure 24.

Table 1. Calibration data.

Detector Position (R) mm	Object Position (A) mm	Voltage (PP) mV
0.000	0.000	330.9
0.127	0.254	328.6
0.254	0.508	328.6
0.381	0.762	328.6
0.508	1.016	324.1
0.635	1.270	320.4
0.762	1.524	319.5
0.889	1.778	314.9
1.016	2.032	312.6
1.143	2.286	311.5
1.270	2.540	306.9
1.397	2.794	305.8
1.524	3.048	303.5
1.651	3.302	303.5
1.778	3.556	302.3
1.905	3.810	301.0
2.032	4.064	298.9
2.159	4.318	292.4
2.286	4.572	291.2
2.413	4.826	289.9
2.540	5.080	282.6
2.794	5.588	269.2
3.048	6.096	263.2
3.302	6.604	249.3
3.556	7.112	239.6
3.810	7.620	227.0
4.445	8.890	199.7
5.080	10.160	197.6
6.350	12.700	181.3
7.620	15.240	173.6
8.890	17.780	157.5

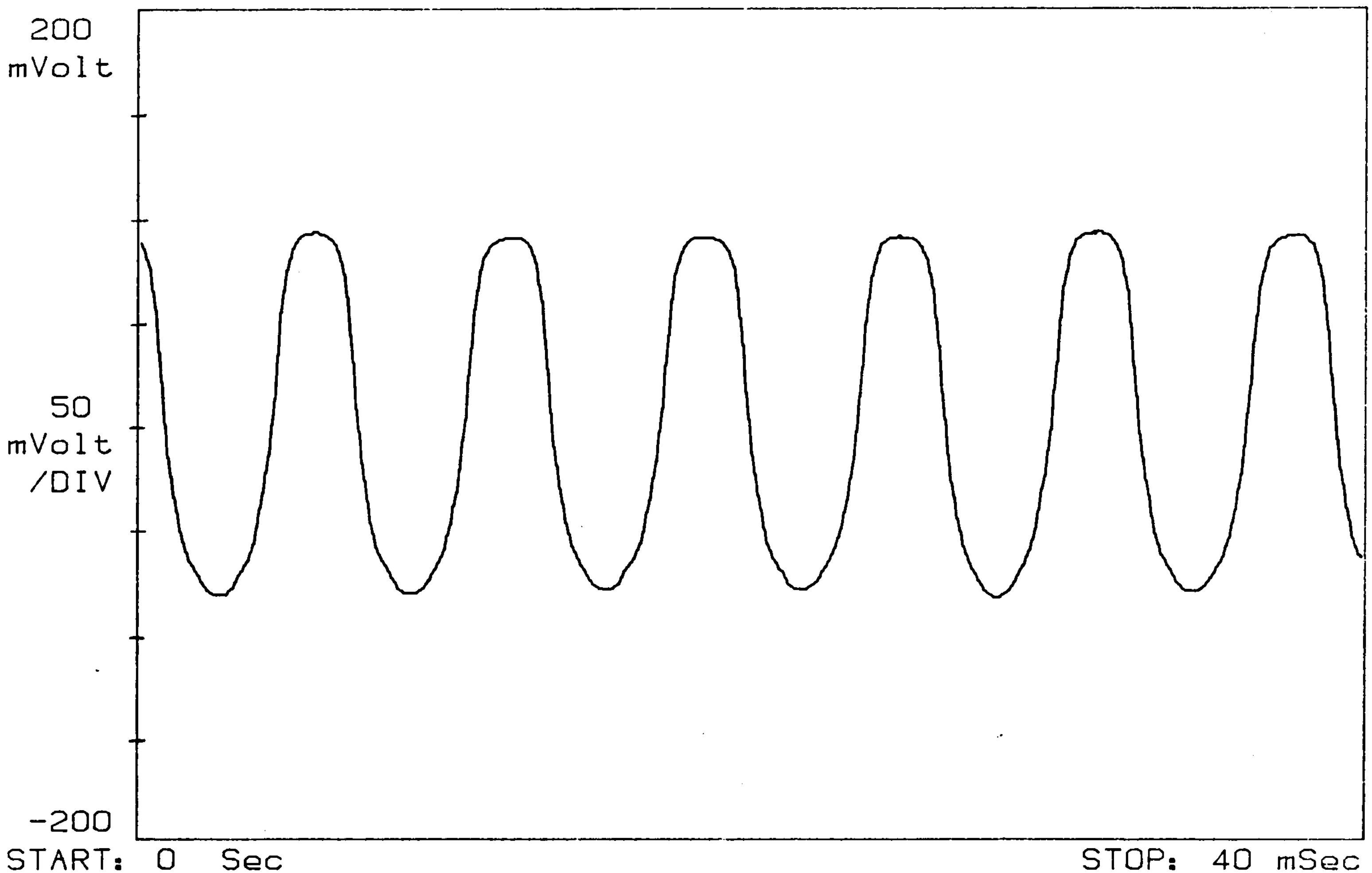

Fig. 16. Detector signal for the upper range.

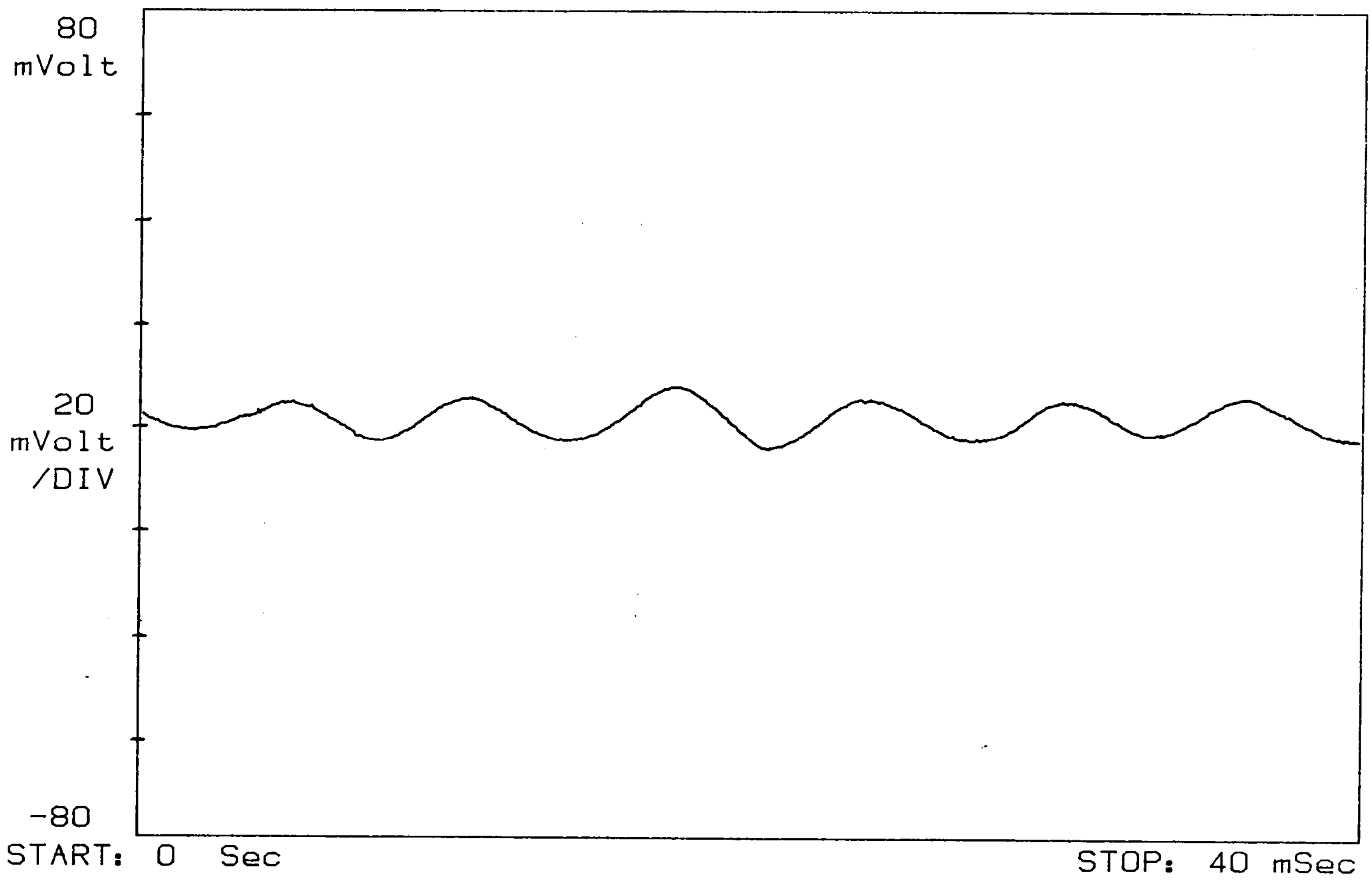

Fig. 17. Detector signal for the lower range.

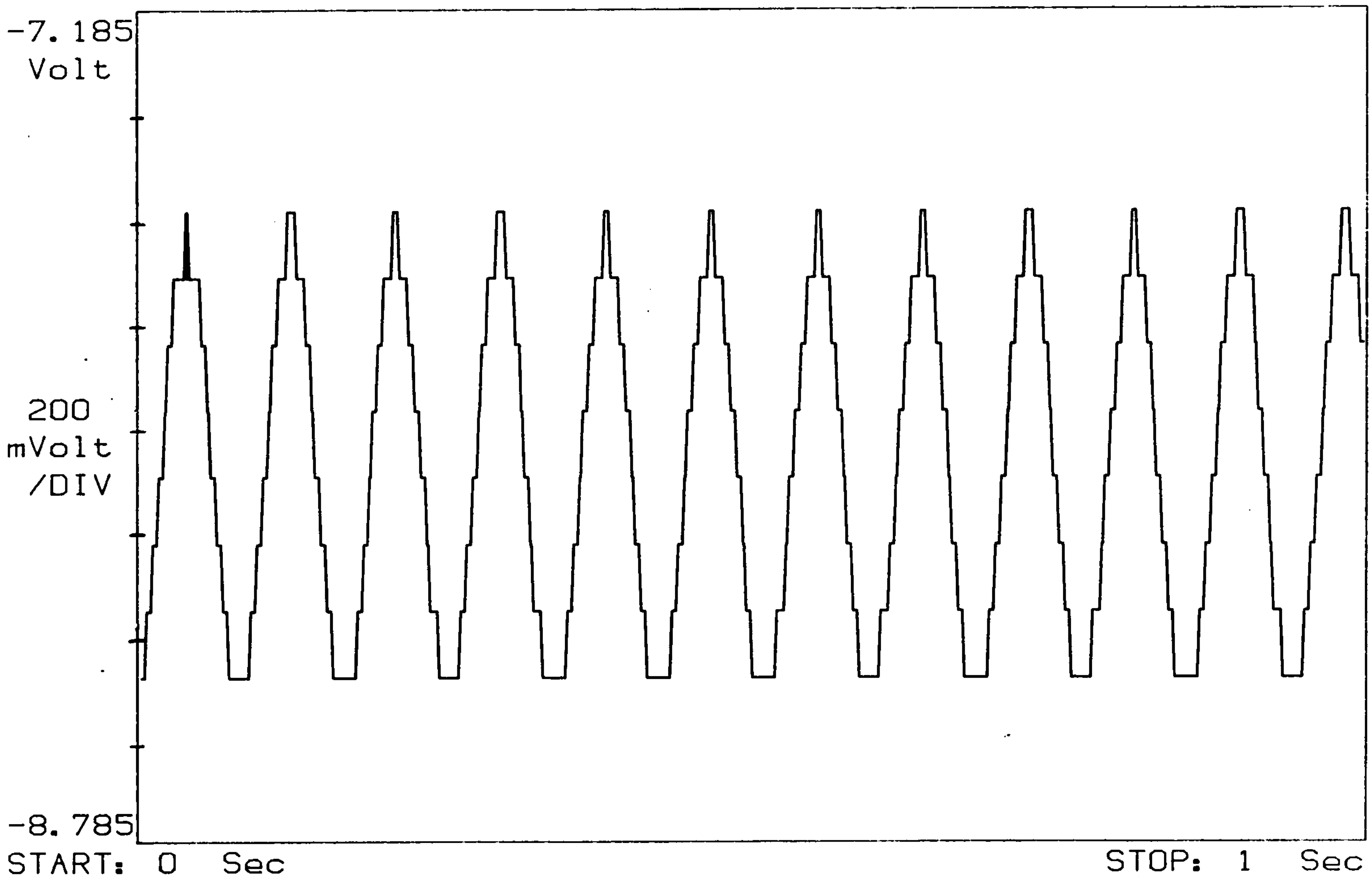

Fig. 18. Input signal for the first mode shape.

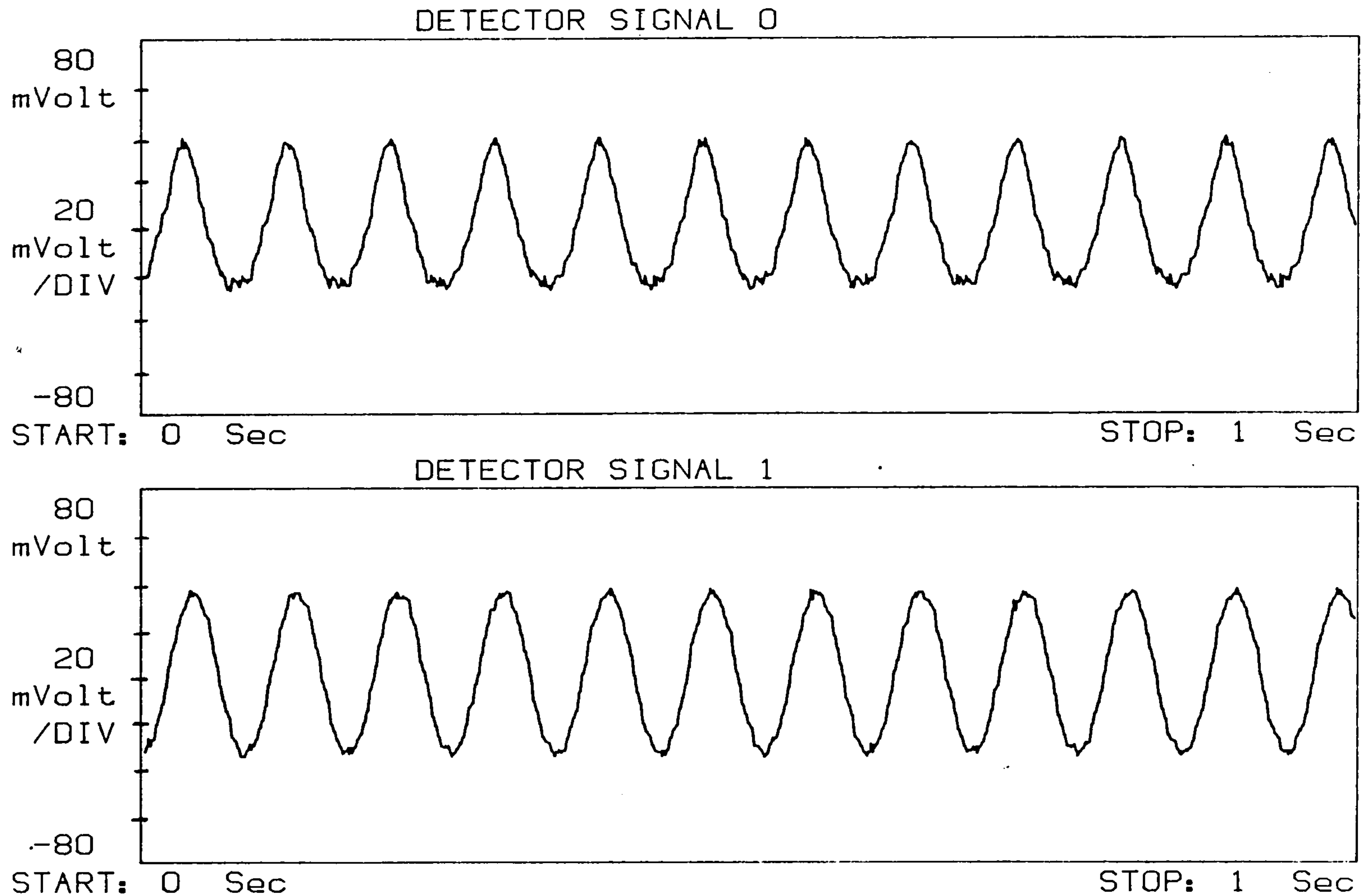

Fig. 19. Detector signals for points 0 and 1, first mode shape.

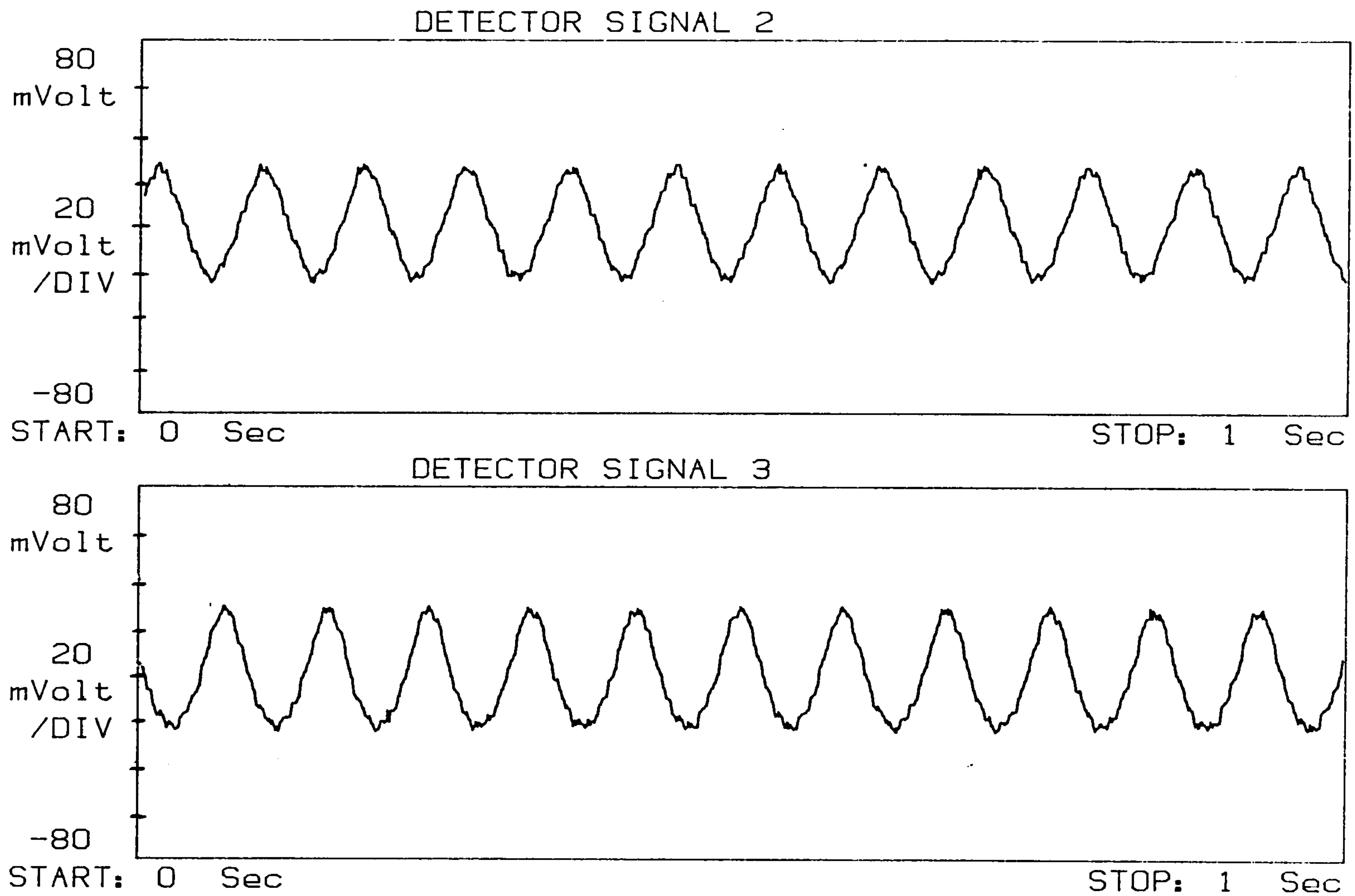

Fig. 20. Detector signals for points 2 and 3, first mode shape.

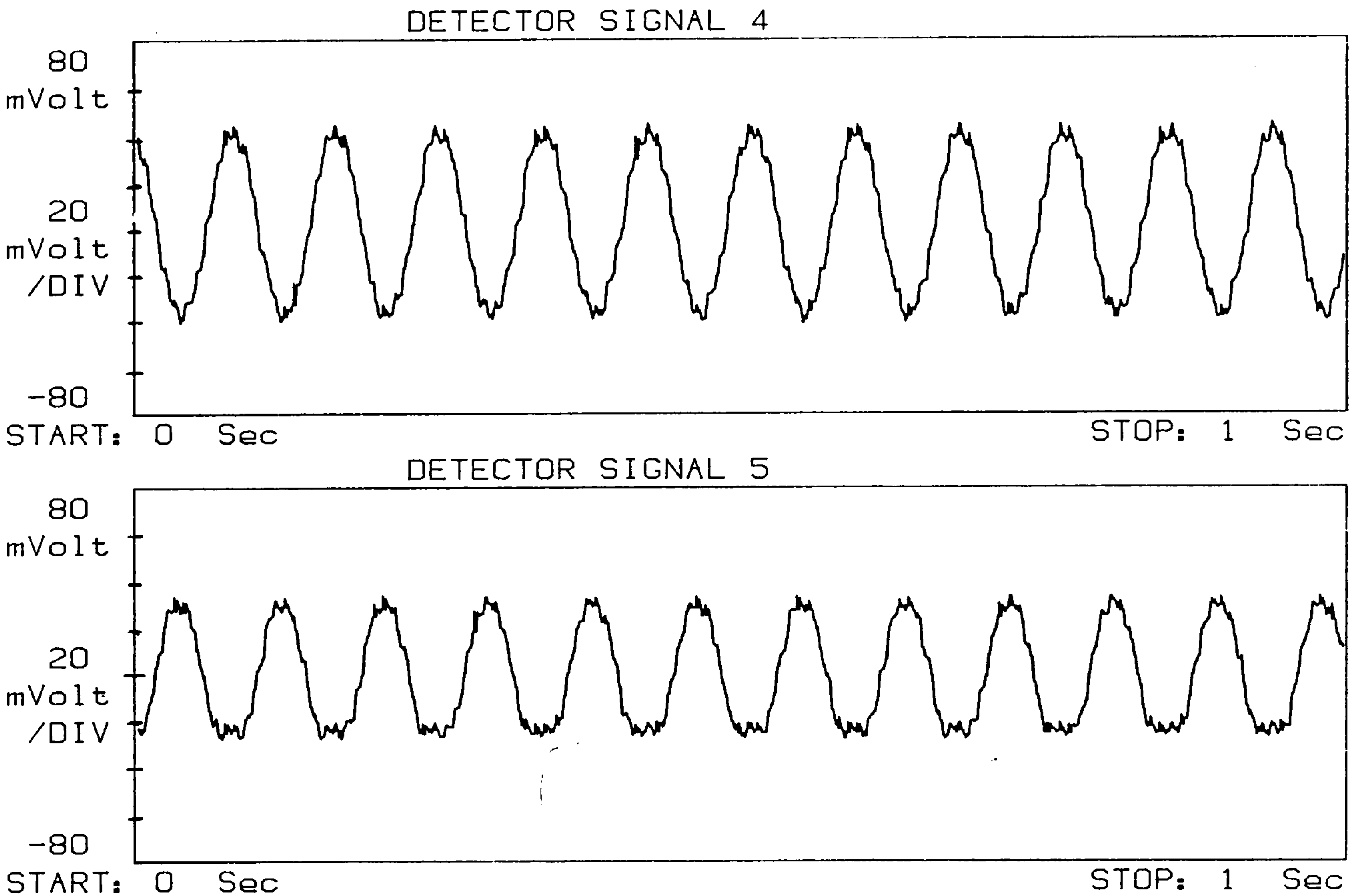

Fig. 21. Detector signals for points 4 and 5, first mode shape.

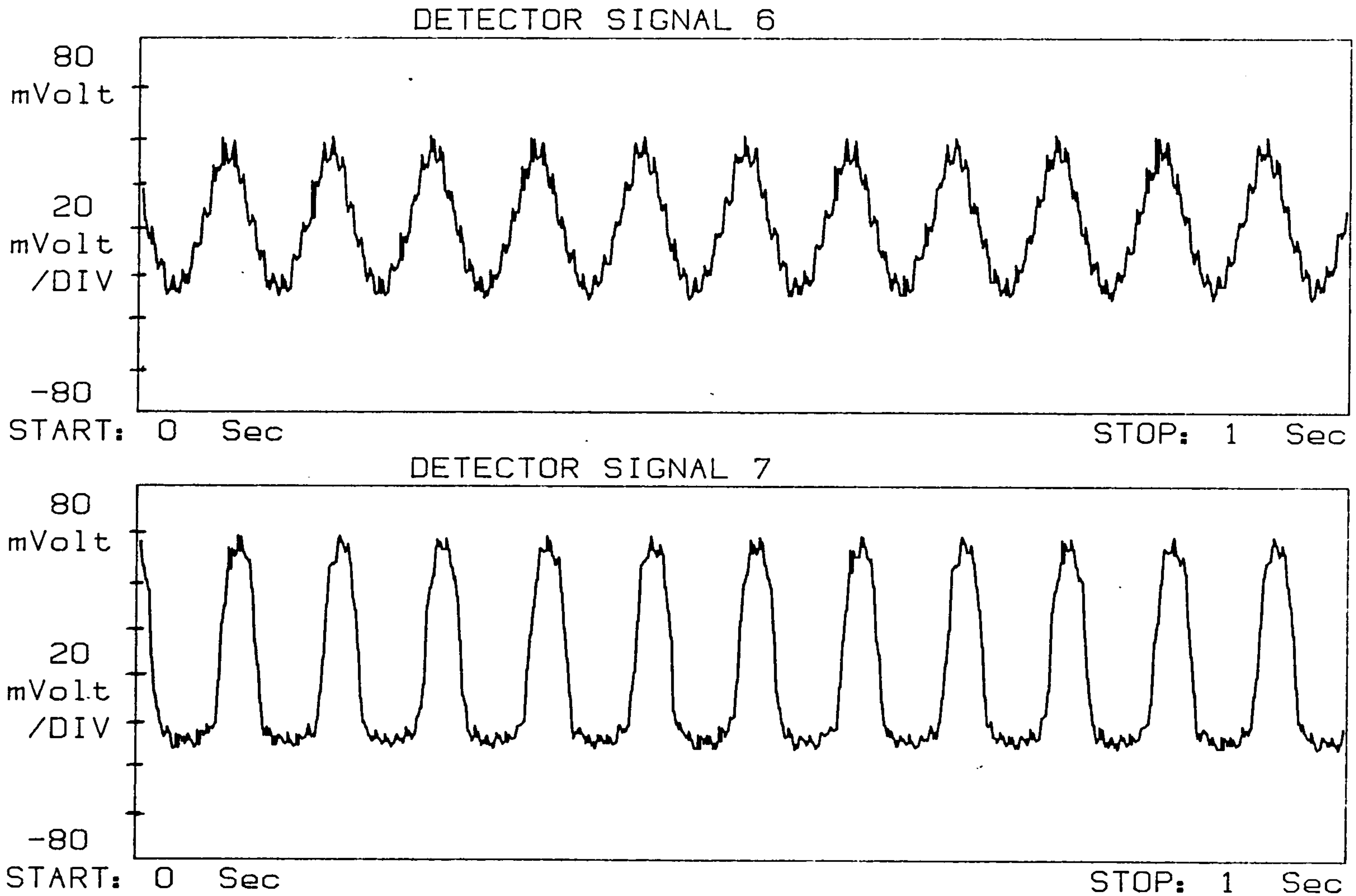

Fig. 22. Detector signals for points 6 and 7, first mode shape.

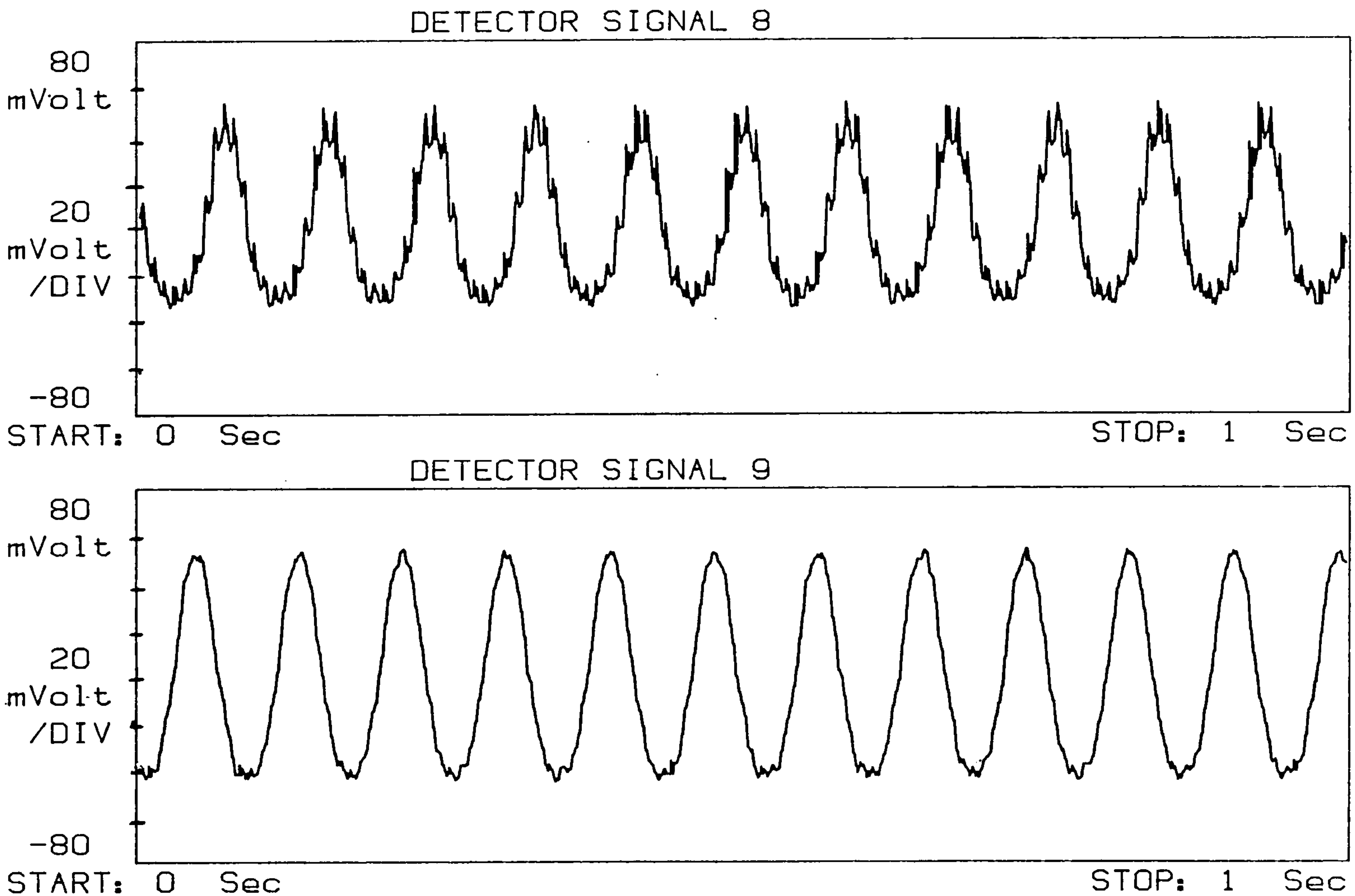

Fig. 23. Detector signals for points 8 and 9, first mode shape.

Table 2. Data for first mode shape.

Point	V_{PP} mV	Vibration Amp. mm
0	62.69	2.9
1	69.83	3.2
2	60.00	2.8
3	65.00	3.0
4	73.59	3.4
5	60.30	2.7
6	68.30	3.2
7	90.21	4.2
8	85.61	4.0
9	95.31	4.4

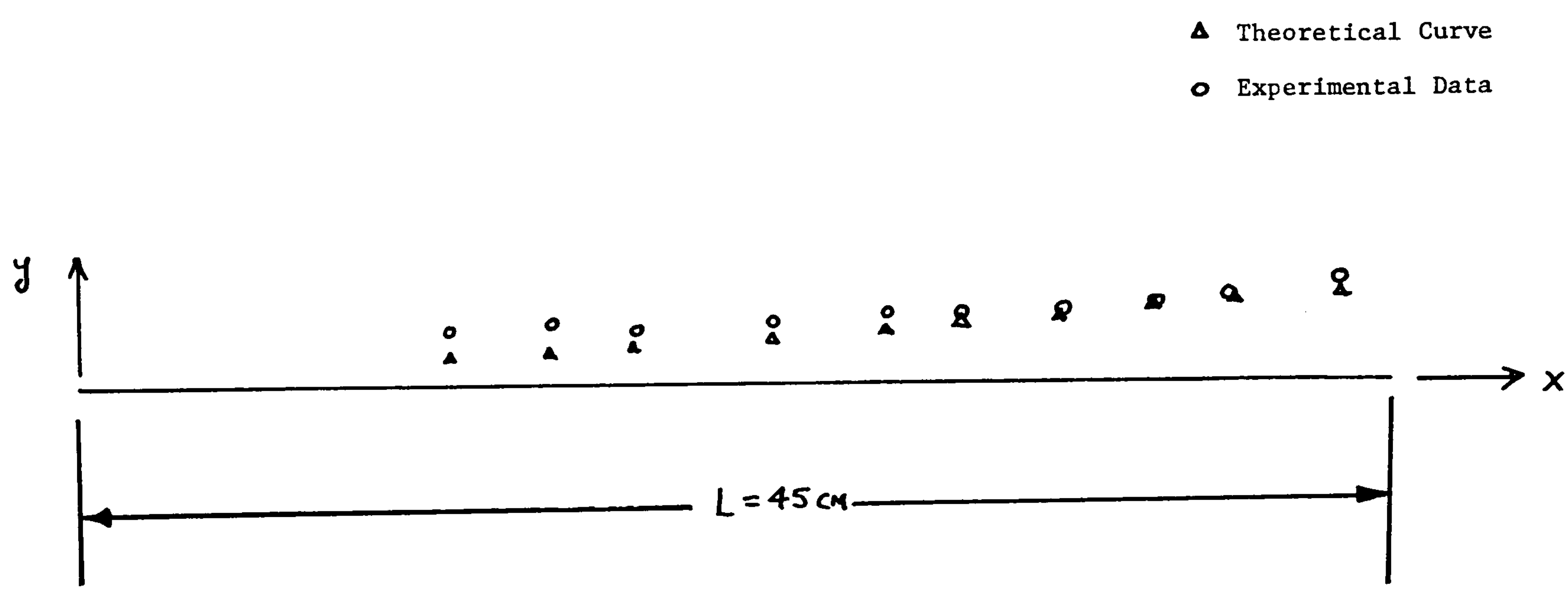

Fig. 24. First mode shape of the cantilever beam.

Figure 25 shows the 155 Hz input signal for the second mode shape. The detector signal amplitudes for each point on the vibrating beam are shown on figures 26 through 30. The voltage readings are converted to vibration amplitude and the data are displayed in Table 3. Figure 31 shows the second mode shape drawn from the data in table 3. This shape correlates well with the theoretical second mode shape for a cantilever beam as shown in figure 31. A good indicator for the validity of this mode shape is the location of the node point. Thomson [4] has tabulated characteristic functions of a clamped-free beam. Table 4 presents a condensed reproduction of Thomson's table. According to table 3, the node point is supposed to occur (linearly interpolating) at 35.10 cm away from the clamped edge. Figure 31 indicates that the mode shape occurs at approximately 31.00 cm away from the clamped edge. This shows a 11.60% difference in the location of the node point.

The third mode shape is determined using the 395 Hz input signal shown in figure 32. The detector signal for each data point is displayed in figures 33 through 37. The voltage reading for each data point is converted to vibration amplitude. These data are presented in Table 5. From these data the third mode shape is drawn. Figure 38 shows the experimental and theoretical third mode shapes. The node points for this mode occur at distances of 21.6 cm and 35.1 cm from the clamped edge. According to Table 6 (condensed from Thomson's theoretical calculation table for the third mode) the node points occur at 22.5 cm and 39 cm from the clamped edge. There is a difference of 4% and 10% in the positions of these node points in the experimental and theoretical determinations.

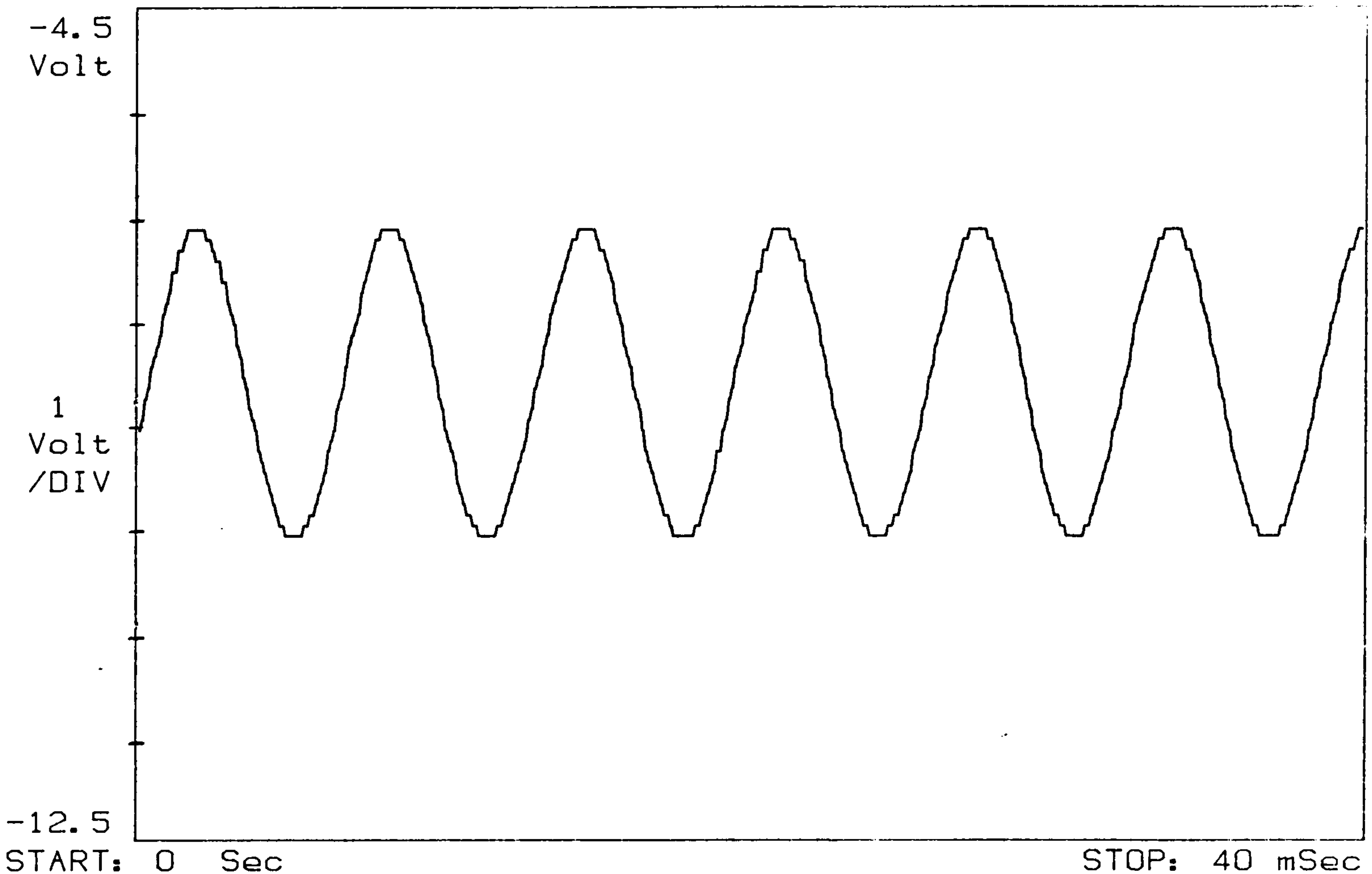

Fig. 25. Input signal for the second mode shape.

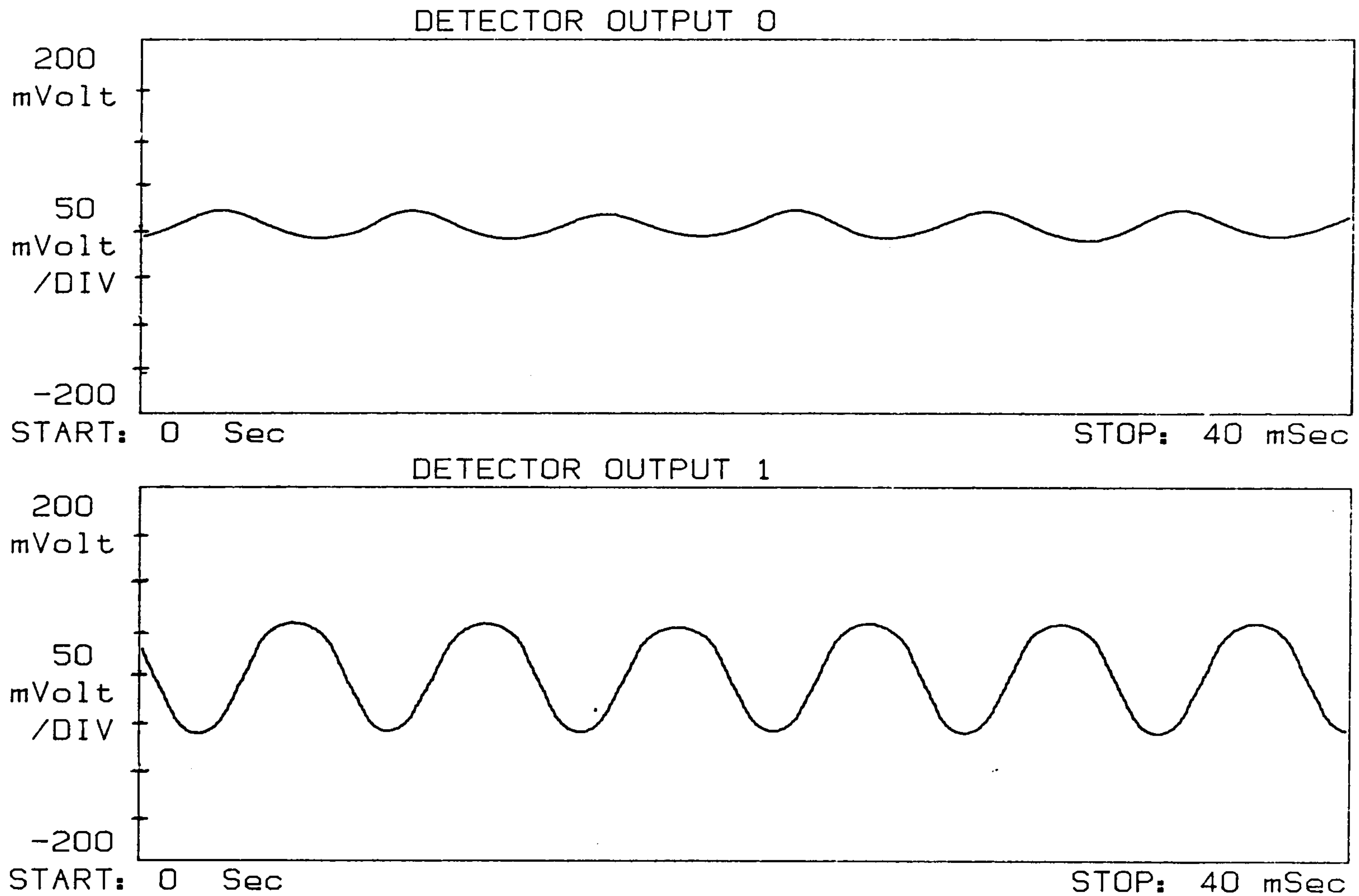

Fig. 26. Detector signals for points 0 and 1, second mode shape.

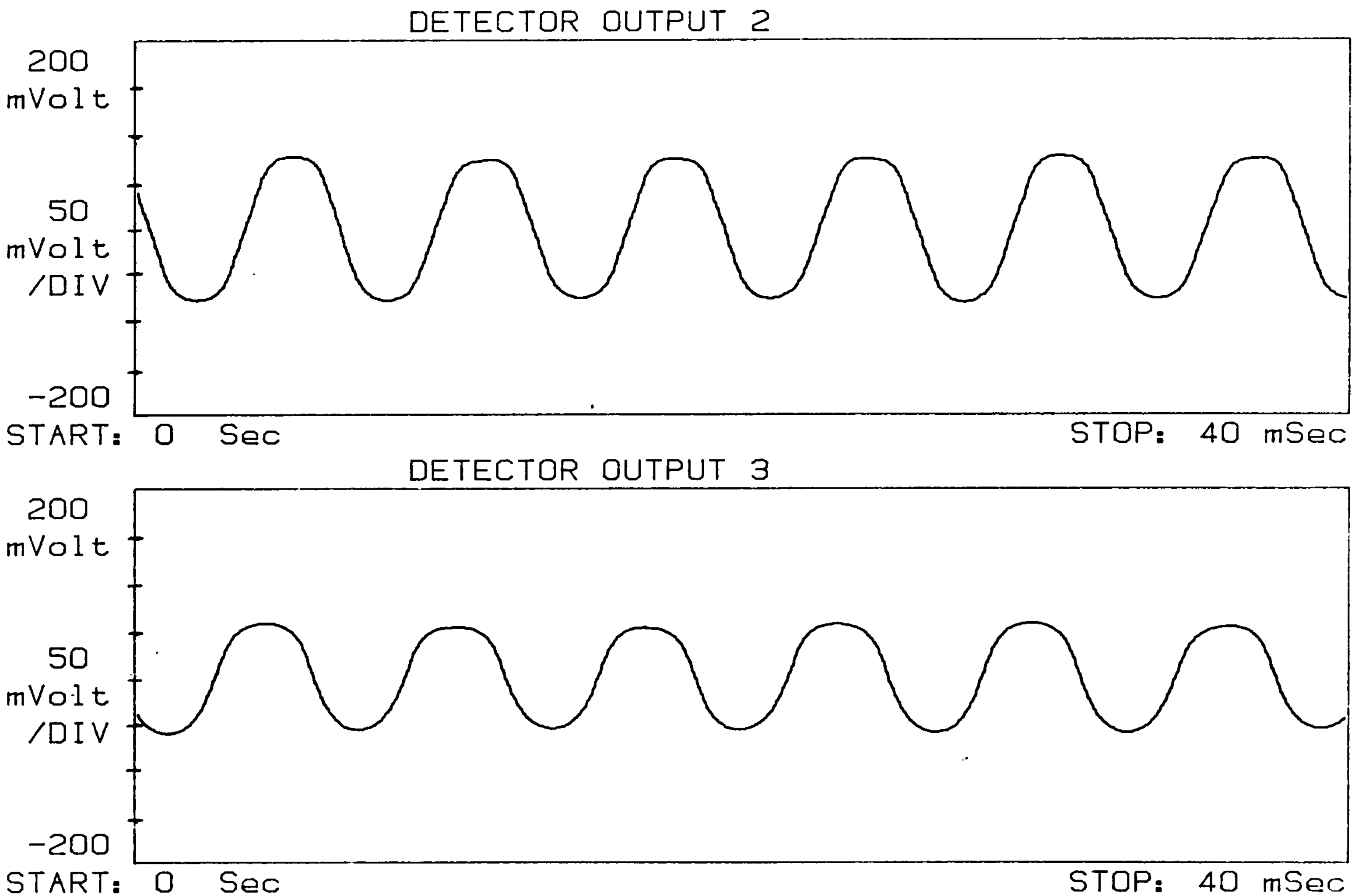

Fig. 27. Detector signals for points 2 and 3, second mode shape.

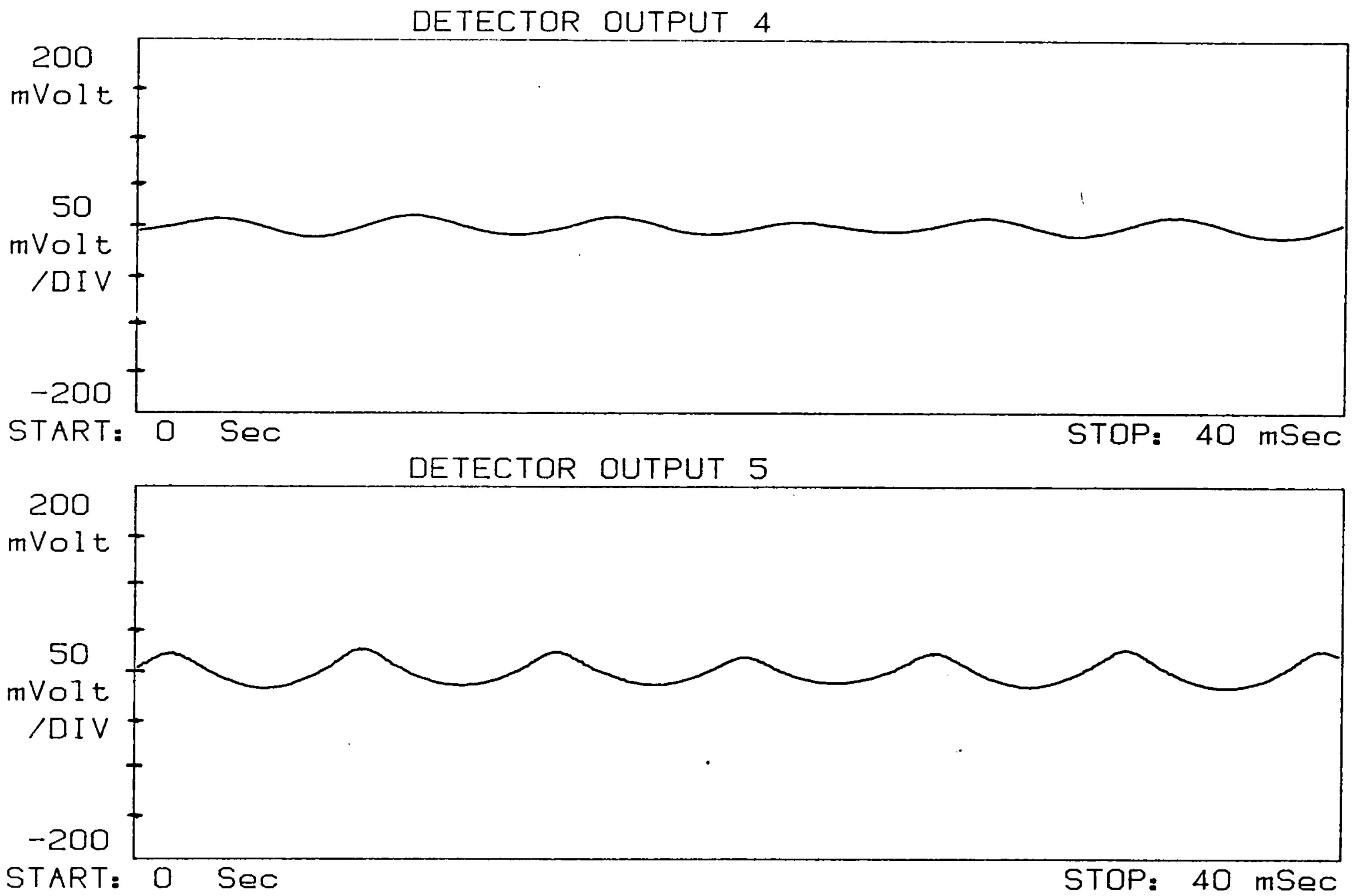

Fig. 28. Detector signals for points 4 and 5, second mode shape.

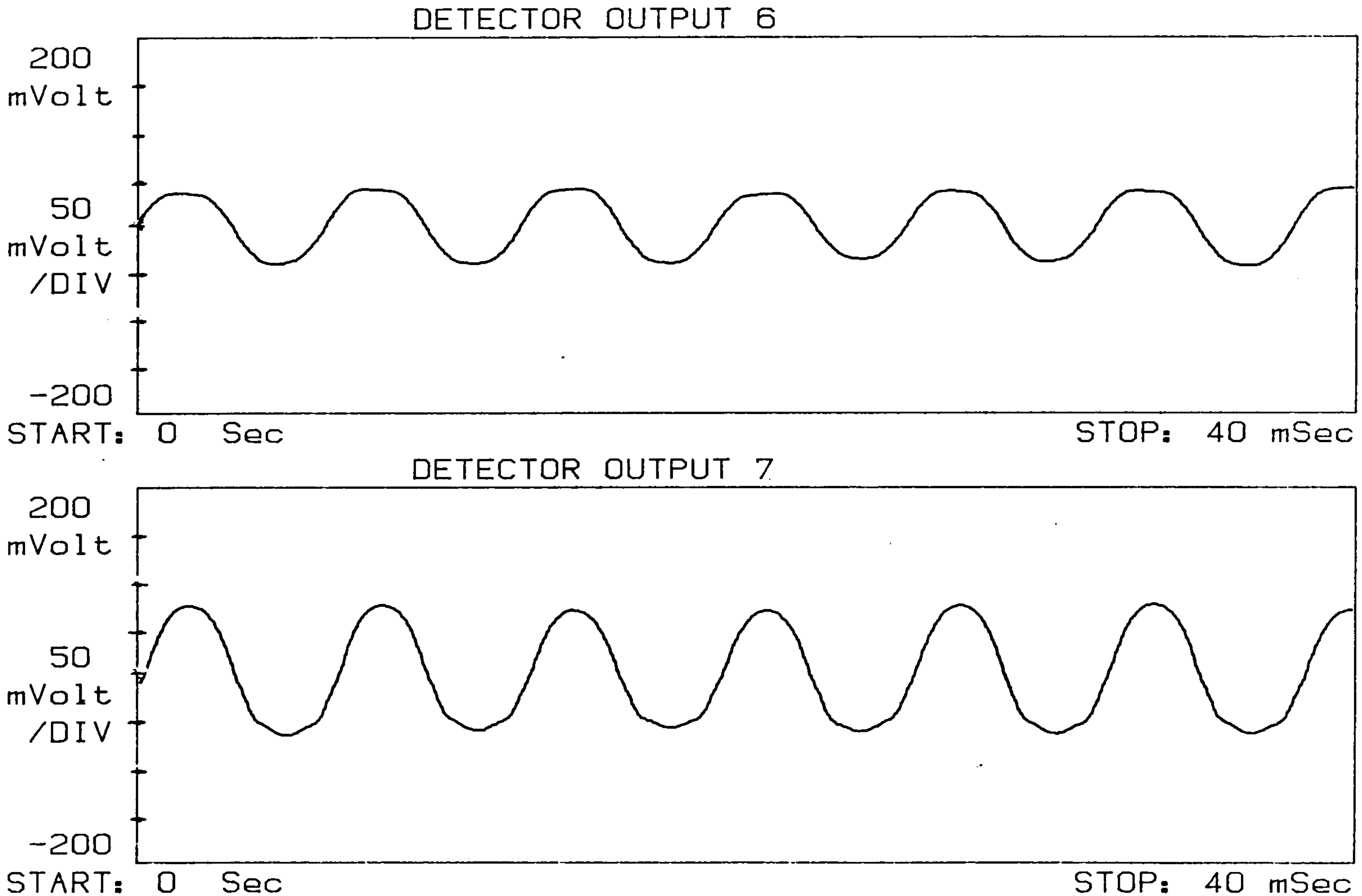

Fig. 29. Detector signals for points 6 and 7, second mode shape.

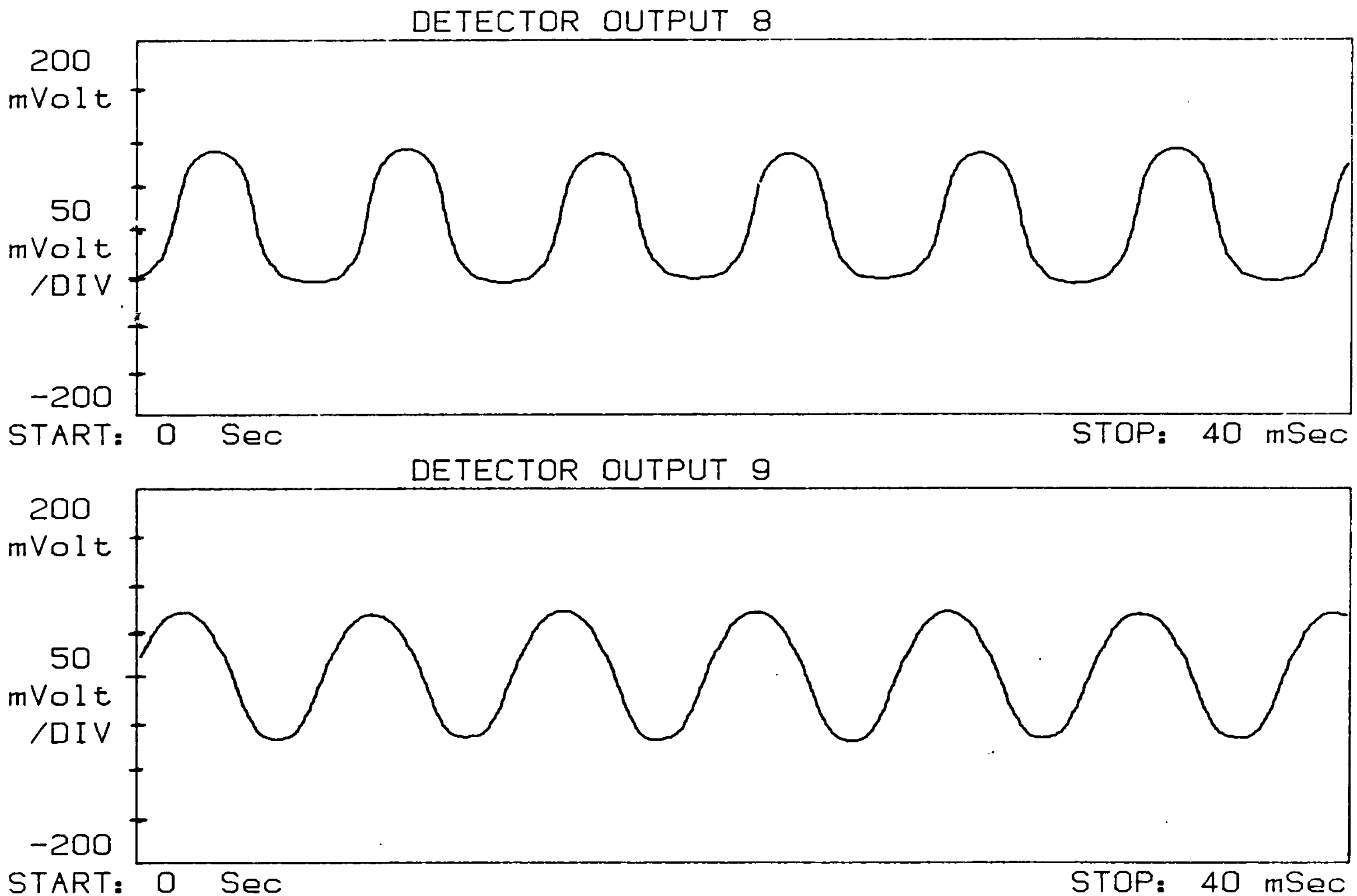

Fig. 30. Detector signals for points 8 and 9, second mode shape.

Table 3. Data for second mode shape.

Point	V_{PP} mV	Vibration Amp. mm
0	29.57	1.4
1	115.70	5.3
2	153.92	7.1
3	108.05	5.0
4	18.875	0.9
5	34.66	-1.6
6	79.00	-3.6
7	133.53	-6.2
8	142.79	-7.0
9	134.56	-6.2

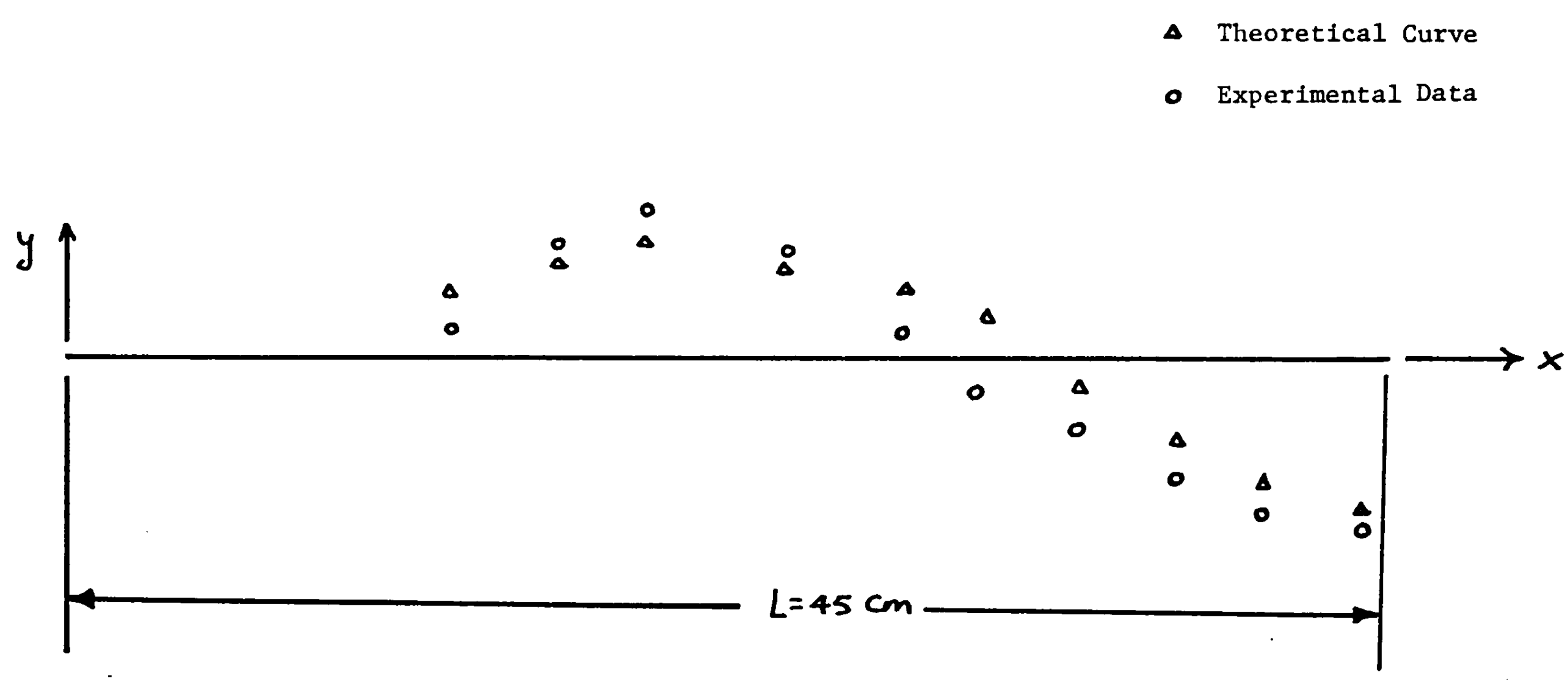

Fig. 31. Second mode shape of the cantilever beam.

Table 4. Characteristic function of a cantilever beam, second mode.

X/L	ϕ_2
0.00	0.0000
0.04	0.03301
0.08	0.12305
0.12	0.25670
0.16	0.42070
0.20	0.60211
0.24	0.78852
0.28	0.96827
0.32	1.13068
0.36	1.26626
0.40	1.36694
0.44	1.48619
0.48	1.43920
0.52	1.40289
0.56	1.31600
0.60	1.17895
0.64	0.99384
0.68	0.76419
0.72	0.49475
0.76	0.19123
0.80	-0.14007
0.84	-0.49261
0.88	-0.86004
0.92	-1.23660
0.96	-1.61764
1.00	-2.0000

ϕ = Characteristic function describing the deqlection.

L = Length of beam.

X = Distance from clamped edge.

Source: William T. Thomson, Theory of Vibrations with Applications, New Jersey: Prentice-Hall, Inc., 1981.

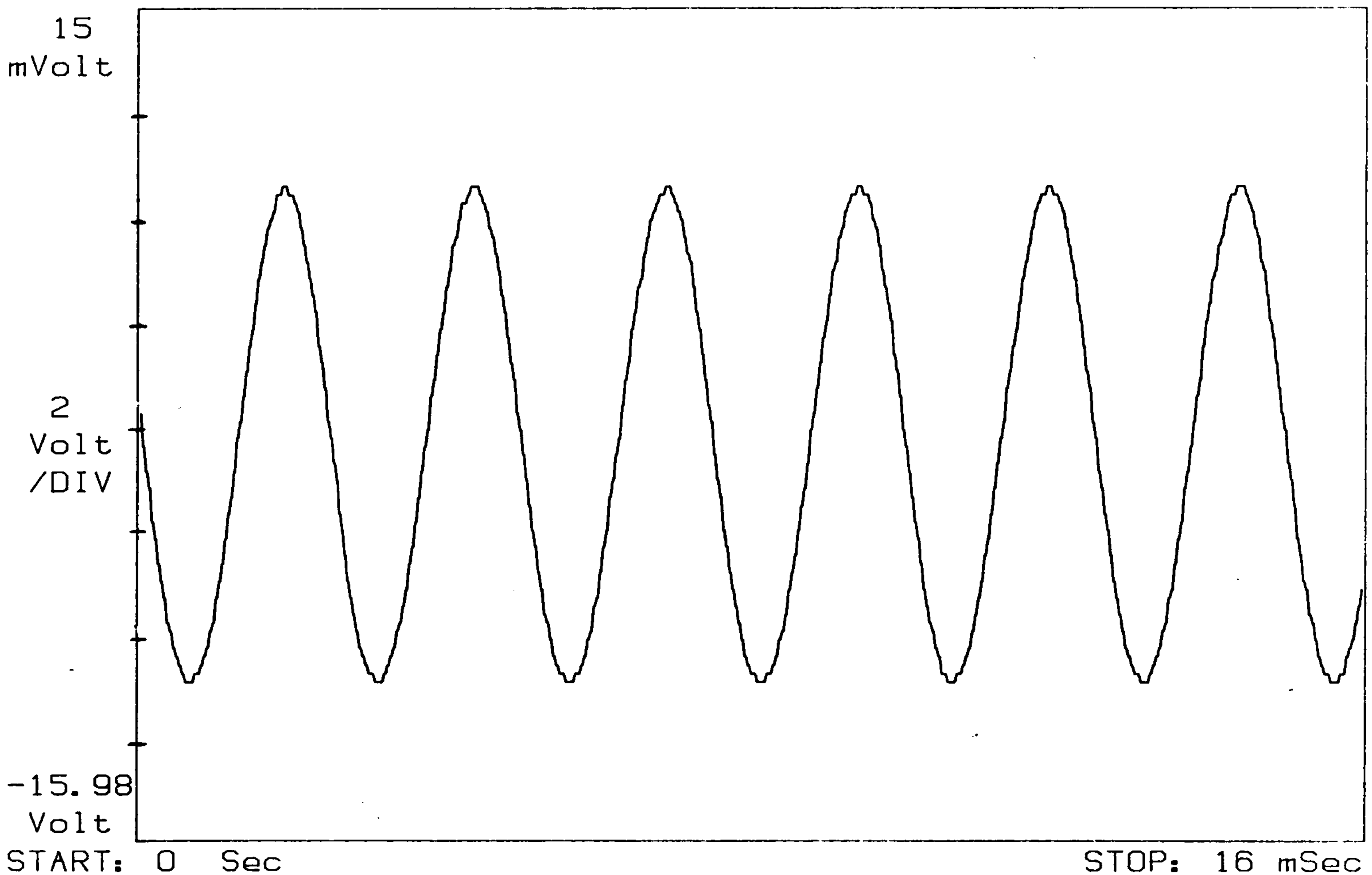

Fig. 32. Input signal for the third mode shape.

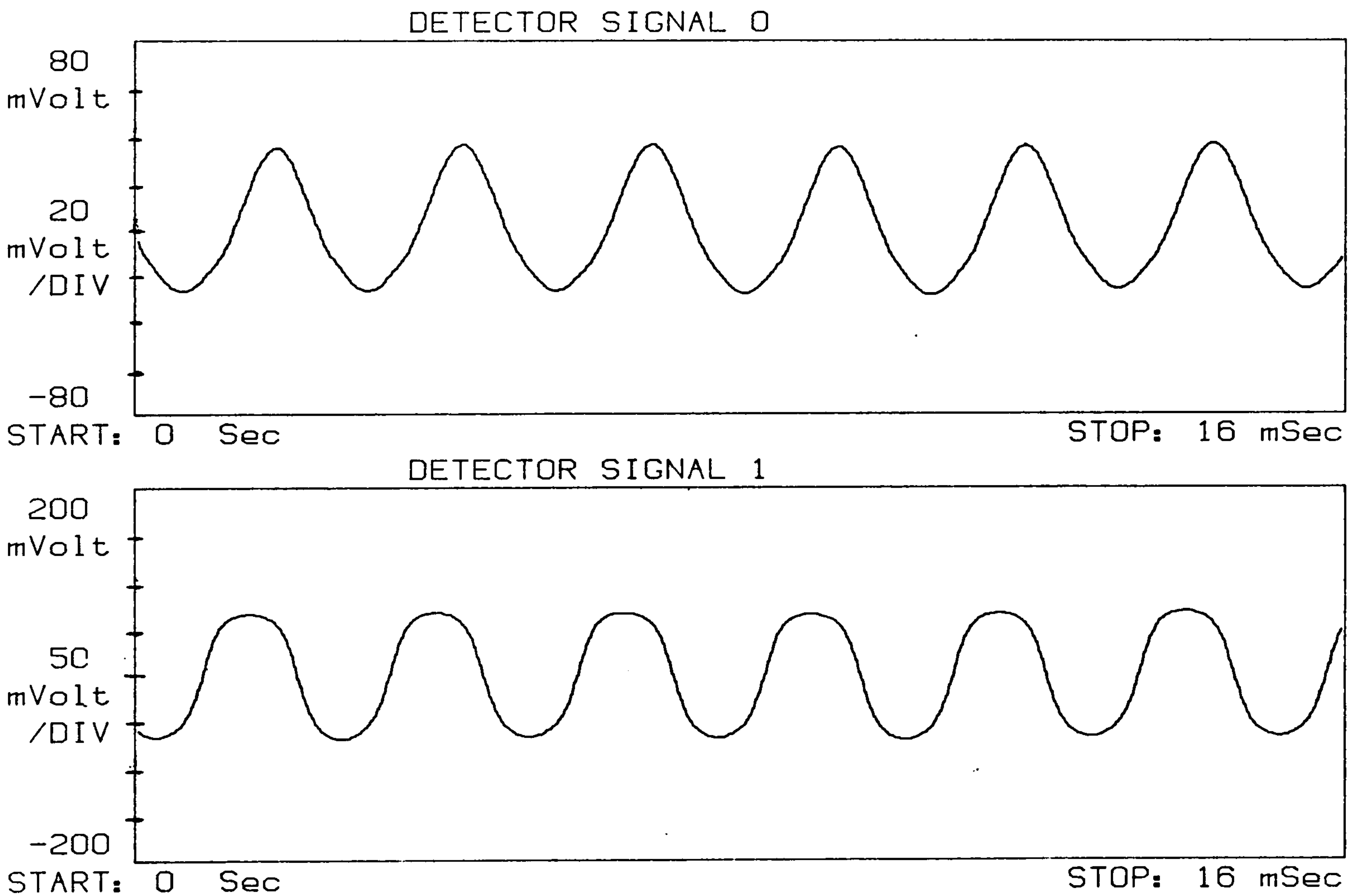

Fig. 33. Detector signals for points 0 and 1, third mode shape.

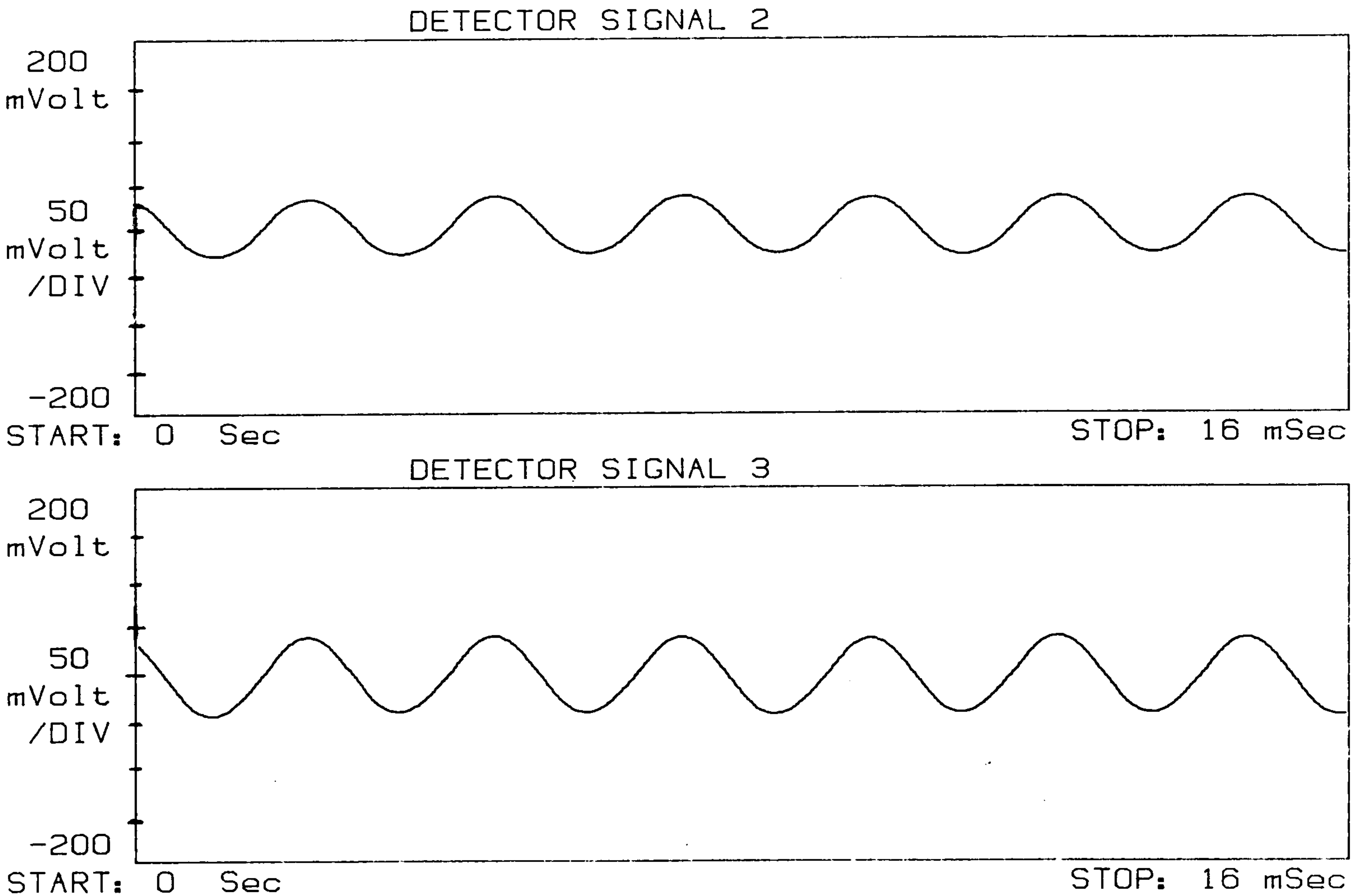

Fig. 34. Detector signals for points 2 and 3, third mode shape.

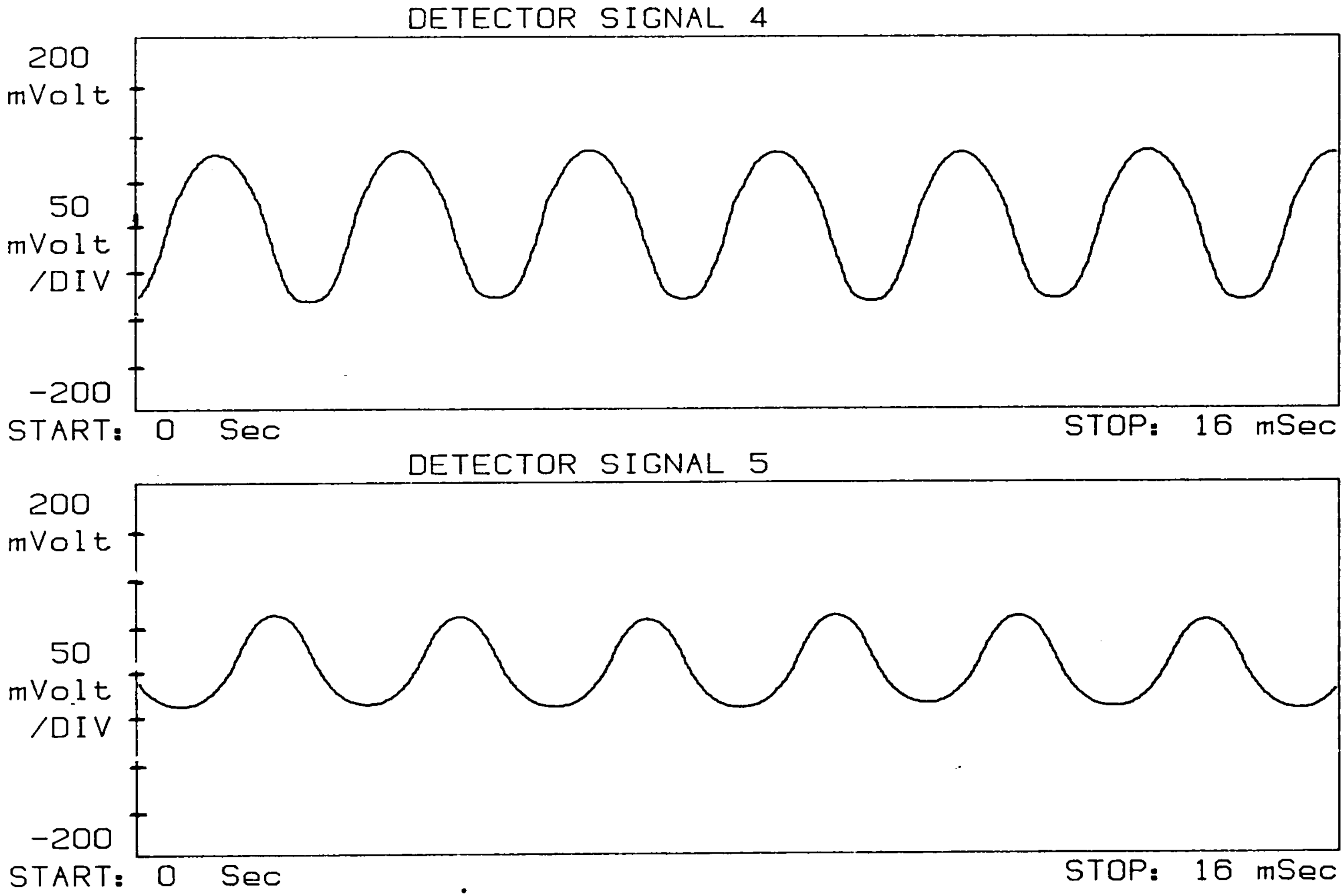

Fig. 35. Detector signal for points 4 and 5, third mode shape.

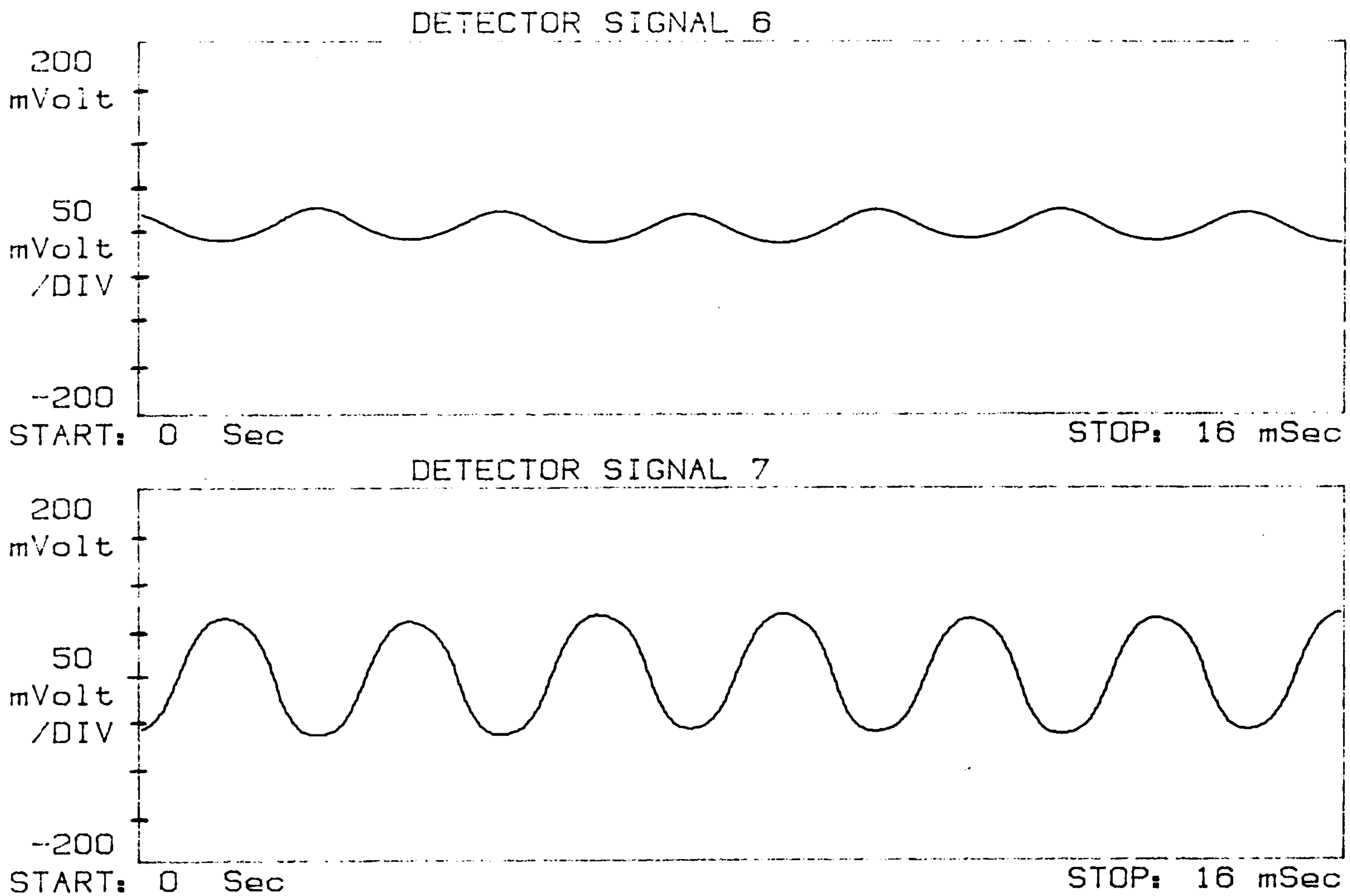

Fig. 36. Detector signal for points 6 and 7, third mode shape.

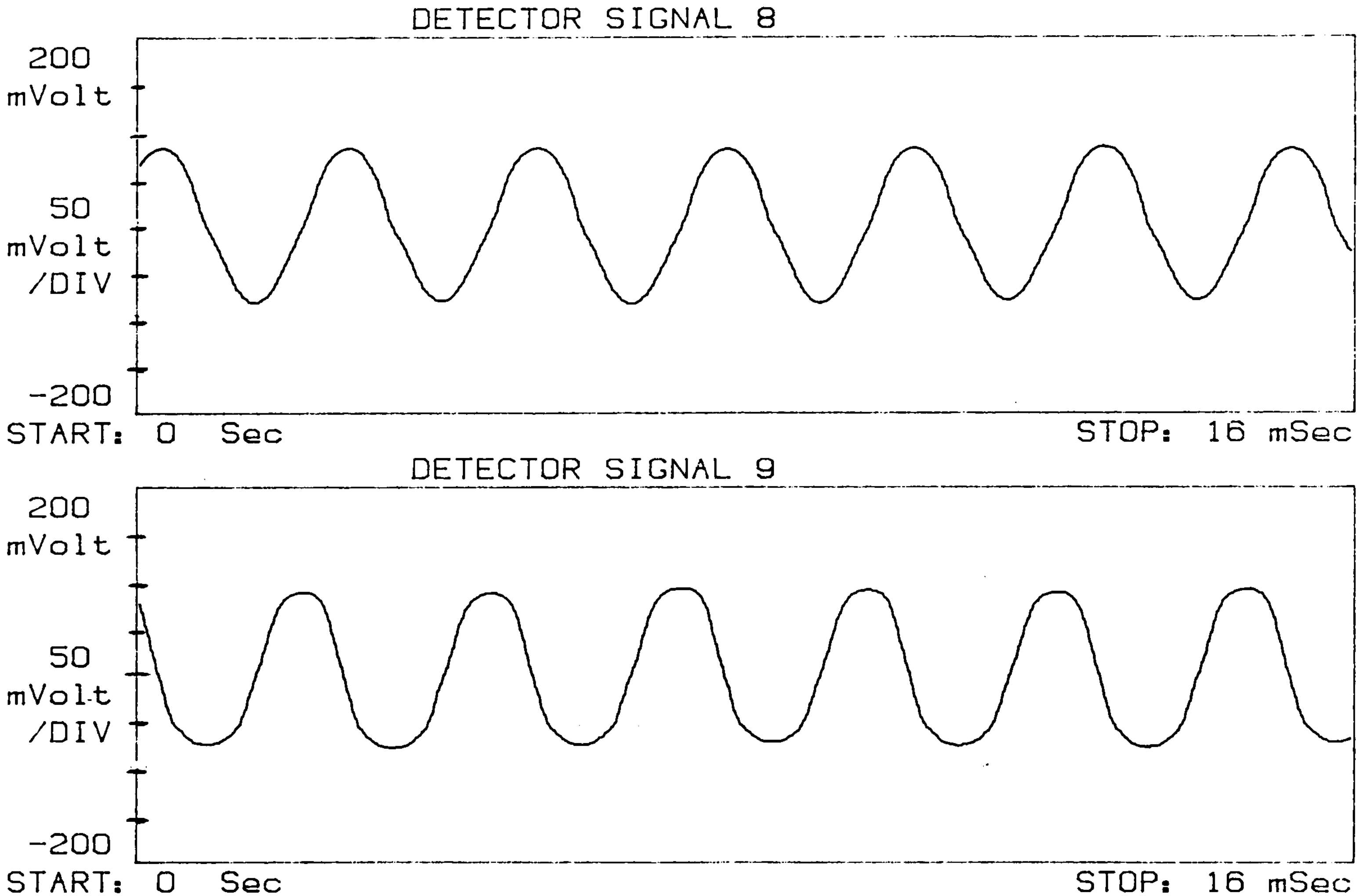

Fig. 37. Detector signal for points 8 and 9, third mode shape.

Table 5. Data for third mode shape.

Point	V_{PP} mV	Vibration Amp. mm
0		
1	132.52	6.1
2	61.16	2.8
3	81.04	-3.7
4	160.04	-7.3
5	99.38	-4.6
6	35.94	-1.7
7	126.4	5.8
8	165.14	7.6
9	162.08	7.5

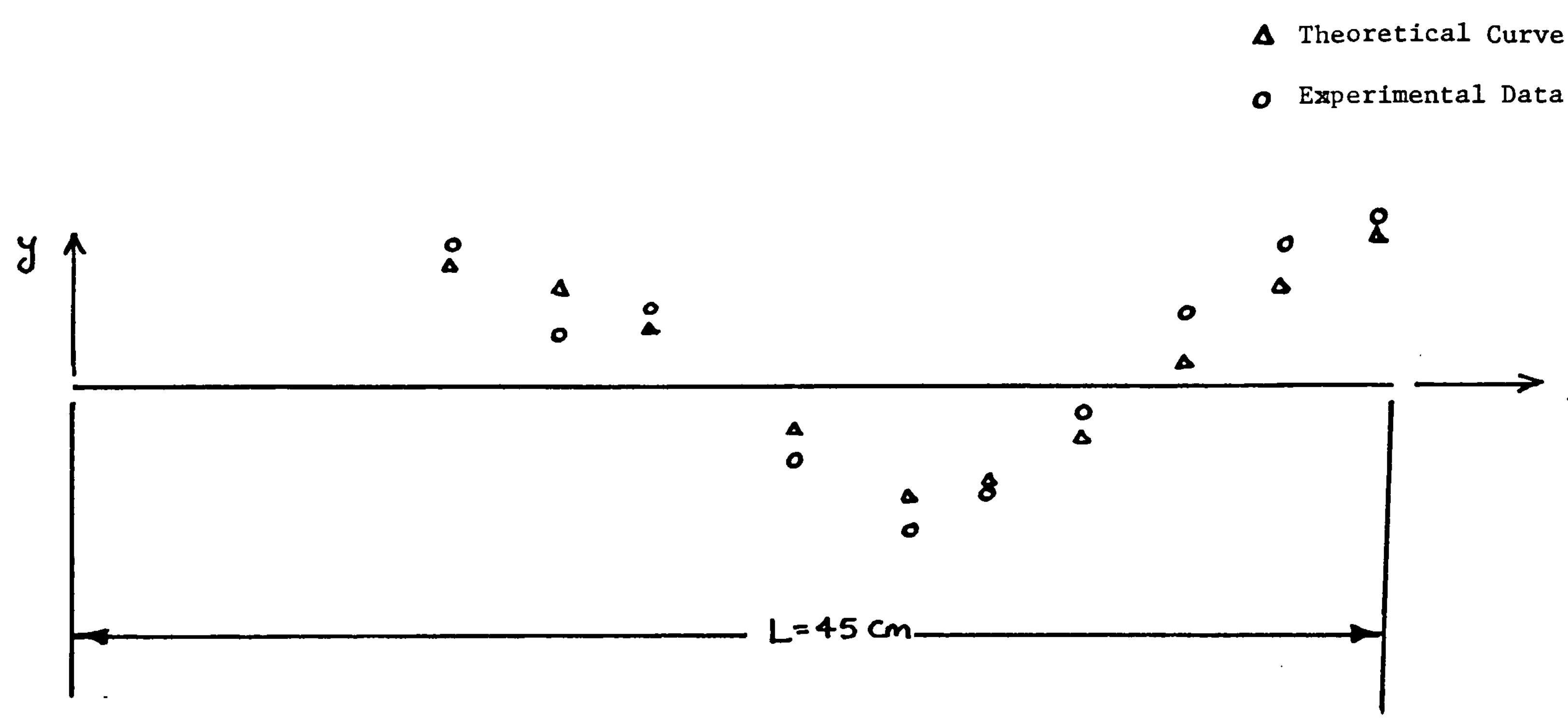

Fig. 38. Third mode shape of the cantilever beam.

Table 6. Characteristic function of a cantilever beam, third mode.

X/L	ϕ_3
0	0
0.04	0.08839
0.08	0.31238
0.12	0.61120
0.16	0.92728
0.20	1.20901
0.24	1.41376
0.28	1.51056
0.32	1.48203
0.36	1.32534
0.40	1.05185
0.44	0.68568
0.48	0.26103
0.52	-0.18130
0.56	-0.59802
0.60	-0.94753
0.64	-1.19398
0.68	-1.31055
0.72	-1.28189
0.76	-1.10515
0.80	-0.78475
0.84	-0.35563
0.88	0.16974
0.92	0.75558
0.96	1.37287
1.00	2.00000

ϕ = Characteristic function describing the deqlection.

L = Length of beam.

X = Distance from clamped edge.

Source: William T. Thomson, Theory of Vibrations with Applications, New Jersey: Prentice-Hall, Inc., 1981.

The difference in the node points for the second and third mode shapes can be attributed to several factors. The most important ones are:

1. The theoretical calculation are based on ideal boundary conditions.
2. Instrument precision error in the experimental setup.

The second factor contributes a larger portion of the error especially for the lower modes. These modes are excited by frequencies that approach the circuit frequency of the ac coupling capacitor of the signal analyzer. Hence, it makes it difficult to accurately reproduce the expected response of the beam at these frequencies.

Conclusions

The technique discussed herein has been determined to be a practical vibration measurement tool. Confidence in this technique is gained as a consequence of correctly tracing the mode shapes of a vibrating cantilever beam. Unlike the existing vibration measurement tools, it has the advantage of being a noncontact procedure. The amplitude measurement range is limited, but improvement of the method should increase the amplitude range that can be measured. Compared to other noncontact methods it has an advantage in its simplicity. The setup requires few components. Lenses, gratings, amplifiers, TV camera, and filters are not required. Since none of these components are used, the use of optical equipment (optical tables and optical mounts) is minimized. This implies that with some modification this setup can be used outside the laboratory environment as long as the environment is not bright enough to interfere with the intensity of the reflected light. Most other noncontact methods such as, moire, holography, and speckle could not be used as easily as the method discussed herein outside the laboratory environment because of stability requirements. In regard to the amplitude measurement range, shadow moire offers a range of 0.1 mm to 100 nm, whereas speckle and holography offer measurement in the interferometric range. However, the method presented in this work allows measurements extending from 0.1 mm to at least 10 mm. Hence, the method discussed herein makes the use of noncontact techniques for objects or structures vibrating within this range possible.

LIST OF REFERENCES

LIST OF REFERENCES

1. Kafri, O., Band, Y. B., Chin, T., Heller, D. F., and Walling, J. C., "Real-time Moire Vibration Analysis of Diffusive Objects," Applied Optics, 24, 1985, pp.240-42.

2. Dirckx, J. J. J., Decraemer, W. F., and Janssens, J. L., "Real-time Shadow Moire Vibration Measurement: method featuring simple setup, high sensitivity, and exact calibration," Applied Optics, 15, 1986, pp. 3785-87.

3. Hecht, E., Zajac, A. Optics, Addison-Wesley, Reading, Massachusetts, 1979.

4. Thomson, W. T., Theory of Vibration with Applications, Prentice-Hall, Inc.,Englewood Cliffs, New Jersey, 1981.

5. Lokberg, O. J., "Electronic Speckle Pattern Interferometry," Phys. Technol. 11, 1980, pp. 16-22.

6. Pedersen, H. M., Lokberg, O. J., Forre, B. M., "Holographic Vibration Measurement Using a TV Speckle Interferometer With a Silicon Target Vidicon," Optics Communications, 12, 1974, pp. 421-26.

VITA

Teodros Belay was born in Asmara, Ethiopia, on October 25, 1963. He graduated, first in his class, from Sanford English Community School, Addis Abeba, Ethiopia, in June 1981.

In March 1985, the Author received a Bachelor of Science in Engineering Science degree from The University of Tennessee, Knoxville. He was initiated as a member in the National Engineering Honor society, Tau Beta Pi, in 1985 and has been a member ever since. He received his Master of Science in Engineering Science degree from The University of Tennessee, Knoxville, in August 1987.